KENNETH FLOYD MARTINEZ. The Design and Evaluation of a Cyclone Sampling Inlet for the Mattson-Garvin Slit-to-agar Bioaerosol Sampler (Under the direction of Dr. Parker C. Reist.)

ABSTRACT

This study focuses on the design and evaluation of a cyclone sampling inlet for the Mattson-Garvin slit-to-agar bioaerosol sampler. Two helical inlet cross-sectional areas were selected based on theoretical estimates that provide a 50% effective cut-off diameter at 8 μm. Cyclone body lengths were selected as multiples (one, two, and three times) of the original sampling inlet diameter. The dimensions of the exit slit were designed to provide a cut-size of 1 μm. Each cyclone configuration was individually placed (side-by-side with a 47-mm filter cassette) in the interior downstream end of an aerosol chamber. Monodisperse aerosol particles, with aerodynamic diameters of 3.6, 5.3, 7, 9.3, and 11.8 μm, of oleic acid tagged with a fluorescent dye (uranine) were generated at the upstream end of the chamber using the Berglund-Liu vibrating orifice monodisperse aerosol generator. The TSI Aerodynamic Particle Sizer was used, at the sampler location, to verify aerodynamic particle size and aerosol generating system operation. The results indicate that the short cyclone body tube length provides the optimum environment for separation of particles, separation efficiency ranged from 15% to 33% for the increasing particle sizes investigated. Helix inlet cross-sectional area had no statistically significant effect on the separation efficiency.

ACKNOWLEDGEMENTS

I would like to extend my gratitude to Drs. Parker Reist, Russell Wiener, and Jerry Tulis for their vision and guidance in the development of this study. Without their knowledge and direction, the completion of this project would have been in serious doubt. Special thanks are given to Charles Frey and the U.S. Environmental Protection Agency (Research Triangle Park, NC) machine shop for their mastery in the construction of the cyclone. I would also like to extend my appreciation to James H. Jones, whose support and confidence in my abilities have helped me to persevere, and to Dr. Dennis O'Brien, who provided me with an informed sounding board upon which I could bounce ideas. In addition, I would like to thank Dr. David Leith (as my academic advisor), C.L. Lassiter, and Carol Carden without whom my education and degree would have never come to fruition.

Finally, but by no means last, I must extend my deepest appreciation and love to my wife Denise and my son Jarrett. For two years, they endured my physical and emotional absence and tolerated my stressed-out personality when I was around. Denise and Jarrett, thanks for letting me come home. Lastly, to my daughter Jennifer, I wished that she could have shared in this experience. Jennifer, I love and miss you. This work is for my family.

TABLE OF CONTENTS

TABLE OF TABLES

TABLE OF FIGURES

LIST OF ABBREVIATIONS

a	molar absorptivity for a sample at an exciting wavelength
ANOVA	analysis of variance
APS	aerodynamic particle sizer
ASHRAE	American Society for Heating, Refrigeration, and Air-conditioning Engineers
b	sample path length along the axis of irradiation
B_o	distance to outlet cylinder wall from centerline
BLCKCAT	variable block category
c	concentration of fluorescing material
C	concentration of the non-volatile solute dissolved in the volatile solvent
cm_3	cubic centimeters
C_o	Cunningham slip correction factor
cfm	cubic feet per minute
d_{50}	50% effective cut-off diameter
D_a	particle aerodynamic diameter generated by VOMAG
d_{crit}	critical diameter for a particle to be separated past the outlet cylinder
d_p	particle diameter
D_p	particle diameter generated by VOMAG
f	frequency
f(Θ)	geometry depending on the effective solid angle
fpm	feet per minute
$g(\lambda)$	response characteristic of the detector
H	height particle will settle over chamber length
H_2O	water
HEPA	high efficiency particulate air filter
I	impurity concentration in alcohol
I_0	exciting radiation intensity
K, N	constants

L	cyclone body tube length
lpm	liters per minute
L_s	chamber length from last baffle to sampler location
ml	milliliter
mm	millimeter
m^3	cubic meters
μg	micrograms
μm	micrometers
MMAD	mass median aerodynamic diameter
N	normal solution
NaOH	sodium hydroxide
nm	nanometers
N_t	number of turns made by gas in cyclone interior
P	pressure drop
pH	concentration of hydrogen ions
PTFE	polytetrafluoroethylene
Q	sampler flow rate
QCEFF0	variable corresponding to the filter cassette and APS ratio minus 1
Q_t	liquid feed rate
Re	Reynolds number
RECEFF	variable corresponding to the cyclone recovery efficiency
RECEFF0	RECEFF minus 1
$(S_f)_\lambda$	sample fluorescence intensity at a given wavelength
SAMPEFF	variable corresponding to the cyclone sampling efficiency
SAMPEFF0	SAMPEFF minus 1
SEPEFF	variable corresponding to the cyclone separation efficiency
Stk	Stokes number
u	air velocity through sampling inlet slit
U	uranine concentration in solution

U_0	maximum velocity for application of still-air sampling criteria
v_o	cyclone inlet velocity
$V_{chamber}$	chamber air velocity
VOMAG	vibrating orifice monodisperse aerosol generator
V_{ts}	particle terminal settling velocity
W	sampling slit half width
w	aerosol chamber width

LIST OF SYMBOLS

τ	particle relaxation time
μ	air viscosity
ρ_p	particle density
π	3.14159
ρ_{avg}	average density of oleic acid and uranine
λ	wavelength
θ	angle
ϕ_f	quantum efficiency of a molecule
ϵ	separation efficiency

I. INTRODUCTION

Bioaerosols have become a prominent safety and health issue with the increased awareness of air quality in indoor environments and its effect on the physical well-being on the occupational work force. However, the hazards associated with bioaerosols have not been limited to indoor environments. The assessment of exposure to infectious microbial agents dates back as far as the study of microbiology. The interest with non-infectious agents (specifically, microbial agents capable of eliciting immunologic responses in susceptible individuals) has only surfaced within the past couple of decades. Human exposure to microbial sensitizing agents have been widely documented in agricultural situations and to a more limited extent in the biotechnology industry (e.g. enzyme manufacturing and citric acid production) [Ström and Blomquist, 1986; Kotimaa et al., 1984; Vincken and Roels, 1984; Topping et al., 1985; Martinez et al., 1988]. With the advent of genetic engineering or recombinant DNA techniques, new interest has focused on the methodologies for sampling bioaerosols to assess risks associated with releases of microorganisms from biotechnology processes.

There are several sampling instruments currently available for assessing the viable microorganism concentration in the ambient air. These samplers include:

- Andersen Viable Cascade Impactor (six-, two-, and single-stage)
- Surface Air Sampler
- Biotest Reuter Centrifugal Sampler
- Slit-to-agar Sampler (e.g. Mattson-Garvin)
- All Glass Impinger

Only the slit-to-agar sampler is capable of producing results that include a time factor. This is useful for assessing exposures from processes or operations that produce periodic peak concentrations of microbial laden aerosols. However, the slit-to-agar sampler is incapable of selective particle size separation (unlike the Andersen six- and two-stage cascade impactors).

The concept was proposed to combine the best attributes of the Andersen and slit-to-agar samplers into a novel bioaerosol sampler design. Two "must" constraints on the design of this "new" sampler were selective particle size separation and a time factor. Preliminary ideas included particle impaction over a series of test tubes individually designed to collect increasing particle size ranges and a rotating agar drum with various sampling inlet designs (i.e. impactor slits or holes, filters, and cyclones) that separate particles into various size ranges (for example, respirable and non-respirable). Due to the focused escalation on the design of a particle size separating inlet, the completion of a working sampler design within practical temporal limits, and the limited available resources, a modified study

proposal was submitted that encompassed the design and evaluation of the sampling inlet for the Mattson-Garvin slit-to-agar sampler. Focusing this study on the sampling inlet removes variability due to other aspects of bioaerosol sampler design (i.e. the design of workable sampling pump and motorized drive systems, the selection of construction materials that facilitates effective sterilization, and the design of a sampling particle impaction media surface or impingement liquid).

The premise behind the operation of the Mattson-Garvin slit-to-agar sampler is based on inertial impaction theory. As a particle laden air stream suddenly changes direction, the inertia of the particles will force them to continue along their original path [Reist, 1984]. The impactor behavior is described by a dimensionless parameter known as the Stokes number (*Stk*):

$$Stk = \frac{u\tau}{W} \qquad (1)$$

where u is the velocity of the air through the slit of the sampling inlet (Figure 1.1), W for rectangular openings is the opening half width, and τ is the relaxation time of an individual particle defined by the following equation:

$$\tau = \frac{1}{18}\frac{d_p^2}{\mu}\rho_p C_c \qquad (2)$$

where d_p is the diameter of an individual particle, μ is the viscosity of the

air, ρ_p is the density of the particle, and C_c is the Cunningham slip correction factor. A rotating base (which holds the oversized plastic petri dish, 15 by 150 millimeter - mm) continually exposes a clean portion of the agar surface to the incoming stream of air. The rotating base allows the continuous enumeration of aerobic bacteria or fungi (based on the nutrient media used) to be assessed over a specific time interval. The continuous enumeration of microorganisms over time is similar to the "real-time" instrumentation being used to assess chemical occupational exposures in industrial settings [Gressel et al., 1988; O'Brien et al., 1989]. Four drive motors of various speeds are provided with the sampler. These drive motors are designed to provide sampling times of 5, 15, 30, and 60 minutes. The sampler is manufactured with an internal pump assembly designed to operate at a flow rate of 28.3 liters per minute (lpm).

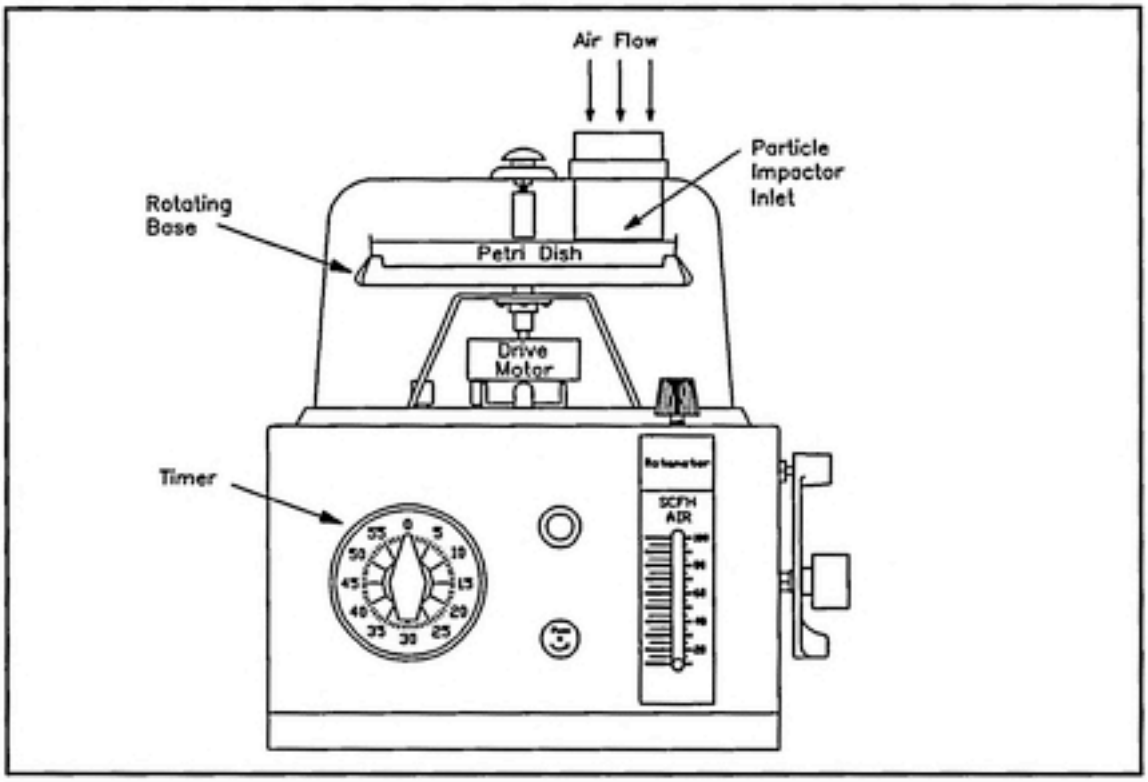

Figure 1.1: Mattson-Garvin Slit-to-agar Sampler

II CYCLONE DESIGN

2.1 Literature Review

A cyclone configuration was selected as the best design for the sampling inlet based on its ability to separate a single air mass, its relative high separation efficiency, and its ease of use (sterilization, cleanup, etc.). Other particle size classification devices were explored including cascade impactors, elutriators, and centripetal devices, but only the virtual impactor and axial inlet cyclone designs retain particle size fractions in the airborne state. A cyclone with an axial inlet and a peripheral discharge was proposed as the final sampling inlet design. Schematics of axial inlet flow cyclone designs (using bladed swirl vanes) are shown in Figure 2.1 [Caplan, 1977]. An extensive review of the literature provided little information on the theories of axial inlet (straight-through) cyclone design. However, a few papers documented successful designs for industrial process and industrial hygiene applications [Vaughan, 1988; Burnard, 1988; Akiyama and Marui, 1989; Walters et al., 1983; Ogawa, 1984; Tenney, 1980]. In some of these case studies, axial inlet cyclone performance empirical models were proposed and formulated. Due to this limited information, the design of an axial inlet cyclone was based on the application of reverse-flow cyclone theories and appropriate empirical models. Several designs must be fabricated and tested (independent of the whole sampling system) to

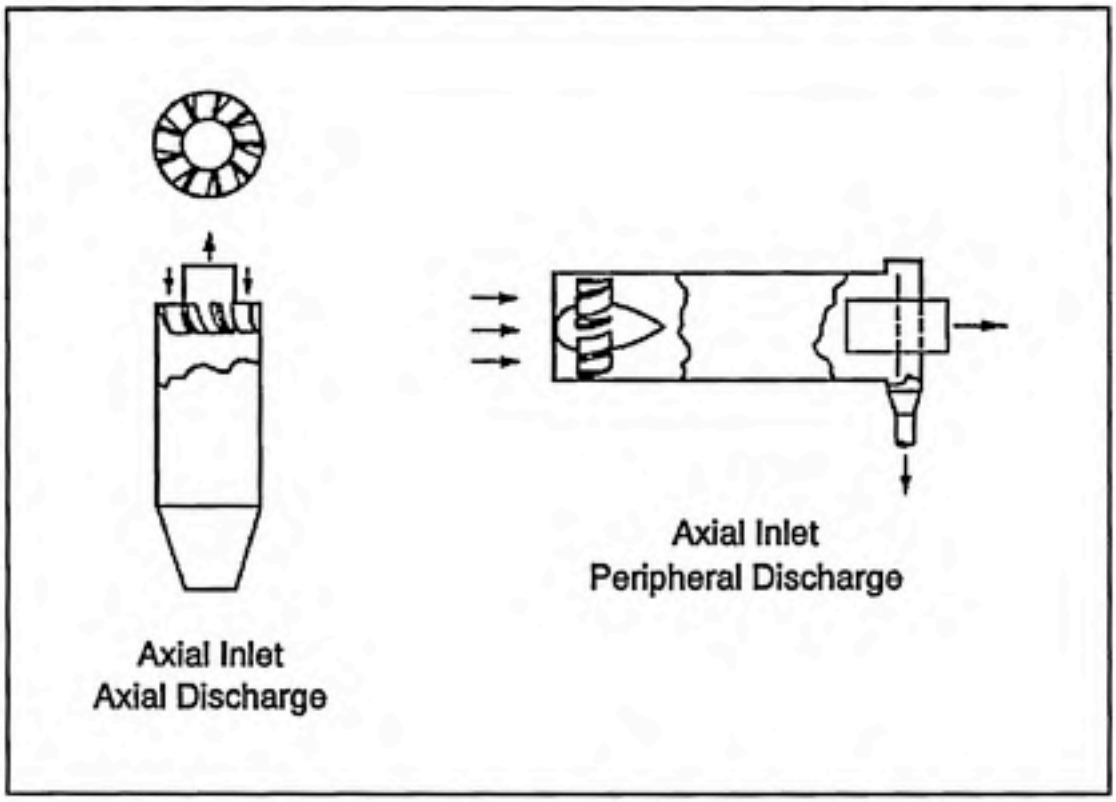

Figure 2.1: Axial Inlet Cyclone Designs

determine the optimum operating conditions for the cyclone that will meet the pre-selected particle cut-size.

Burnard, Walters et al., and Akiyama and Murai proposed cyclone designs based on the use of turning vanes to induce a rotational component to the flow of an incoming gas. Burnard evaluated four variations of the same cyclone design which is compatible with the MRDE high capacity dust collector varying spinner hub diameter, spinner blade number and pitch, cyclone diameter and length, and outlet tube diameter and length. Increasing the number and/or the pitch of the spinner blades increased the efficiency

and resistance of the system (the effect diminished progressively). Collection efficiencies ranged from 85% to 95% for 6 to 12 blades 70 millimeters (mm) in width. Reducing the spinner hub diameter improved the efficiency of the system while reducing air resistance. Variations of cyclone and outlet tube diameters and lengths produced only marginal effects. It should be noted that the designs of Burnard's systems included a water spray nozzle prior to the entrance to the cyclone.

Walters et al. describes an axial flow cyclone designed to separate the liquid water from clouds sampled by aircraft. Walters et al. notes that the turning vane outlet angle is the controlling parameter for the amount of water collected. Specifically, the more the flow is turned the greater the streamwise acceleration and the greater the associated pressure drop. Walters et al. theoretically examined the drop separation based on a critical diameter of 5 micrometers (μm). Virtually all liquid water content reached the duct wall within 1/4 of the distance between the vanes and the extraction slot.

Akiyama and Murai describes an enhancement to the axial flow cyclone design that increases the swirl flow inside the cyclone. Akiyama and Murai's design includes eight nozzles set on the duct wall which induces a secondary air flow tangentially into the main cylindrical duct. Guide vanes were limited to angles of 25° and 45° with varying nozzle angles of 15°,

25°, 35°, and 45°. The cyclone was challenged with four dusts (lycopodium, glass beads, fly ash-5, and fly ash-10) under controlled conditions. Akiyama and Murai noted that large guide vanes generate swirling flow more efficiently than small ones - less pressure drop. In addition, the optimum duct length related to collection efficiency (as swirl flow decays exponentially with axial distance) appears to be approximately three times the diameter of the duct. The critical particle diameter (100% collection efficiency) for the designed cyclone is approximately 10 μm for fly ash-5 and 15 μm for the glass beads. The cut size (50% collection efficiency) is approximately 4 μm for the fly ash and the glass beads.

Vaughan describes an axial flow cyclone design using a thin helical turning vane as opposed to the previous designs that used a series of blades to induce a rotational component to the incoming air flow. The evaluation included a number of variations of the cyclone design namely helix configuration, body length, and flow rate. Chamber length had a considerable effect on the collection efficiency, with the shorter chambers giving higher collection efficiencies. Vaughan notes that for its size, at a given flow rate, the axial flow cyclone design exhibits higher collection efficiencies than the tangential flow cyclone design. Penetration curves for a given axial flow cyclone configuration were extremely sharp. Based on the penetration curves the following relationship was formulated for the 50% effective cut-off diameter (d_{50}):

$$d_{50} = \frac{K}{Q^N} \quad (3)$$

where K and N are constants and Q is the flow rate. Attempts to correlate the observed with the entry velocity or the Reynolds number met with limited success. However, Vaughan proposed a more reliable (± 20%) relationship between the d_{50} and the pressure drop of the system P:

$$d_{50} = \frac{17.64}{\Delta P^{0.44}} \quad (4)$$

Vaughan used flow visualization techniques of the internal processes of the cyclone to explain qualitatively the results of the evaluations. Fluorescently tagged aerosols and coal dusts were used to show where the bulk of material came to rest within the cyclone. From the visualization techniques it appears that the air exiting the helical channel executed a single turn within the length of the cyclone. In addition, at higher flow rates, a distinct ring of deposit was observed around the center underside of the helix insert.

Based an assessment of the literature, the cyclone design described by Vaughan (helical versus bladed turning vane design) would provide the most efficient fractionation of the respirable and non-respirable particles entering into the modified sampler inlet. In addition, Vaughan's concept of a helical insert is conceptually easier to machine (for the small scale required for the modified sampling inlet) than the bladed vane design. The final separating

inlet design specifications were based on theoretical design concepts and the ability to machine various parts of the helical insert and the exiting slit.

2.2 Cyclone Design Criteria

Information related to the design of axial flow cyclones are limited to isolated case studies which, in some cases, provide empirical theories on the performance of such systems. However, it is possible to apply simple cyclone theory as an initial approximation of the axial flow system design. In a typical cyclone, particle bearing ambient air is introduced radially into the upper section of the cyclone chamber causing a rotational component to be added to the incoming flow of air. This rotational component will accelerate particles in the air outward, by their inertia, to the chamber wall. Larger particles will occupy the zone closer to the chamber wall while smaller particles remain entrained in the vortex closer to the centerline of the chamber. Based on certain parameters, the point of separation of respirable and non-respirable particle size ranges can be predicted in the cyclone chamber [Reist, 1984].

Assuming that a gas moves through the cyclone chamber as a rigid air stream with a spiral velocity equal to the average velocity at the inlet, the critical diameter (d_{crit}) for a particle to be separated past the outlet cylinder is given by [Reist, 1984]:

$$d_{crit} = \sqrt{\frac{9 B_c \mu}{\rho_p v_c N_t \pi}} \quad (5)$$

where B_c is the distance to the outlet cylinder wall from the centerline, μ is the viscosity of the air, ρ_p is the density of the particle, v_c is the cyclone inlet velocity, and N_t is the number of turns made by the gas in the cyclone chamber.

Based on this theoretical approach, estimates were made for a range of helix inlet area dimensions capable of velocities (based on a flow rate of 28.3 lpm and an entry angle of 45°) that produce the desired 50% effective cut-off diameter of 8 μm. This cut-off diameter was selected to duplicate the cut-off diameter for the Andersen two-stage viable impactor (designed to produce respirable and non-respirable fractionations [Andersen Samplers, Inc., 1976]). Two inlet areas were selected based on these estimates and the practical limitations of the machining process. Cyclone body lengths were selected as multiples (one, two, and three times) of the original sampling inlet diameter. The diameter of the outlet tube was chosen at random. The dimensions of the exit slit (designed to provide a cut-size of 1 μm) are a function of the Stokes number (Equation 1) describing the impaction of aerosol particles in an air stream interrupted by an obstacle. A 45° taper was added between the outlet tube and the exit slit to produce

stable air streams into the slit and reduce the loss of particles to the bottom of the cyclone.

The cyclone was constructed in sections so that varied configurations could be achieved by "puzzling" together the appropriate sections. Each section was machined of aluminum. Air tight connections were maintained through rubber O-rings around the interior connection point. An aluminum support unit was designed to fit over the cyclone base to hold a 47-mm filter. Photographs of the combined cyclone sections, wide helical insert, and the exit slit base unit are shown in Figures 2.2 through 2.4. A labeled schematic of the combined cyclone sections is provided in Figure 2.5 and the dimensional specifications are provided in Table 1.1.

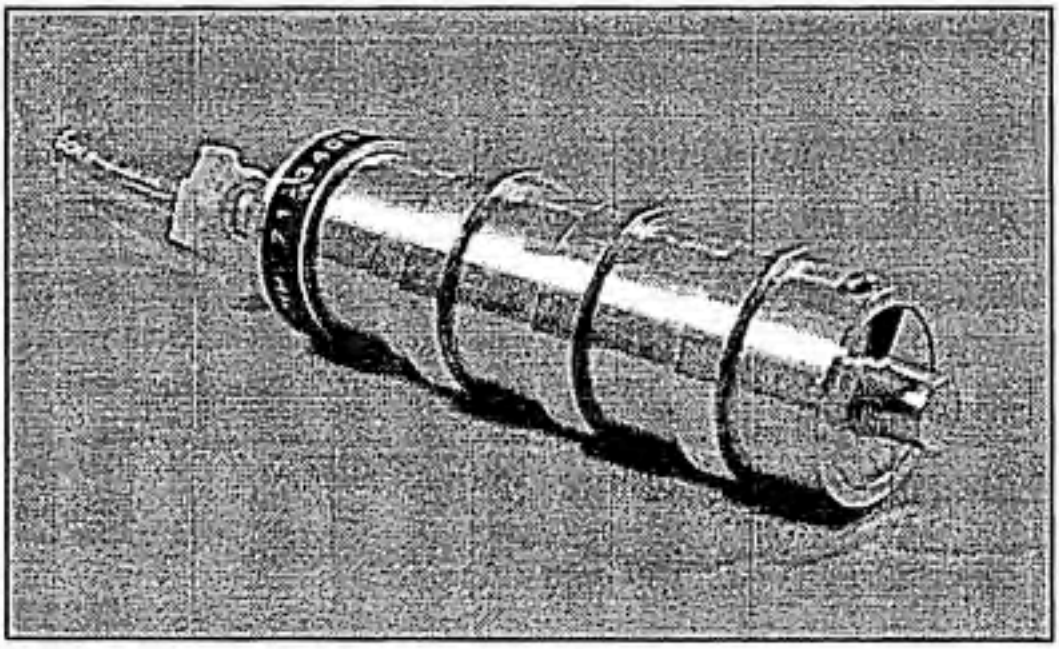

Figure 2.2: Combined Cyclone Sections

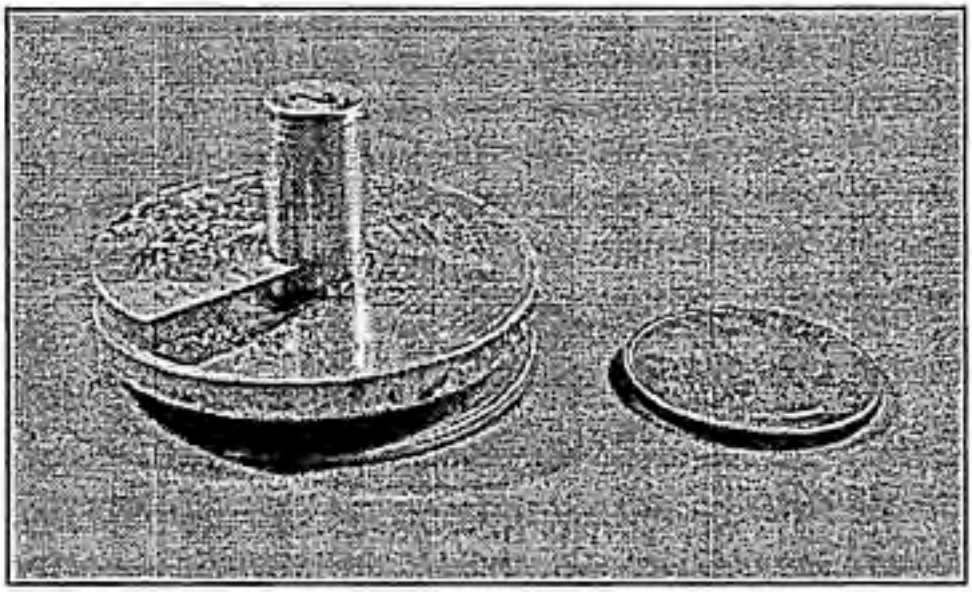

Figure 2.3: Wide Helical Insert

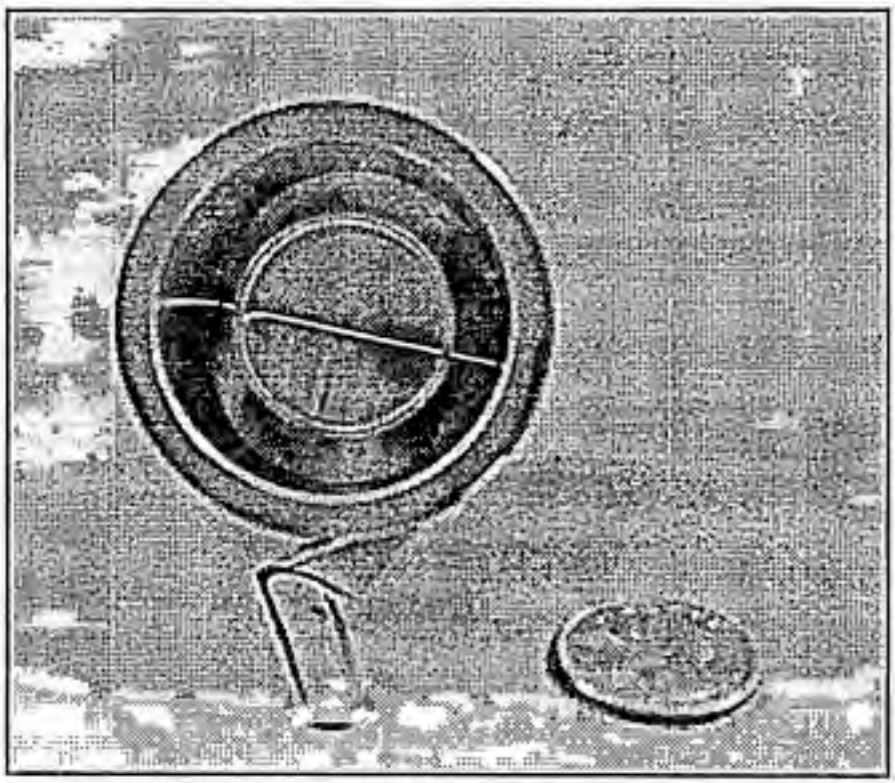

Figure 2.4: Exit Slit Base Unit

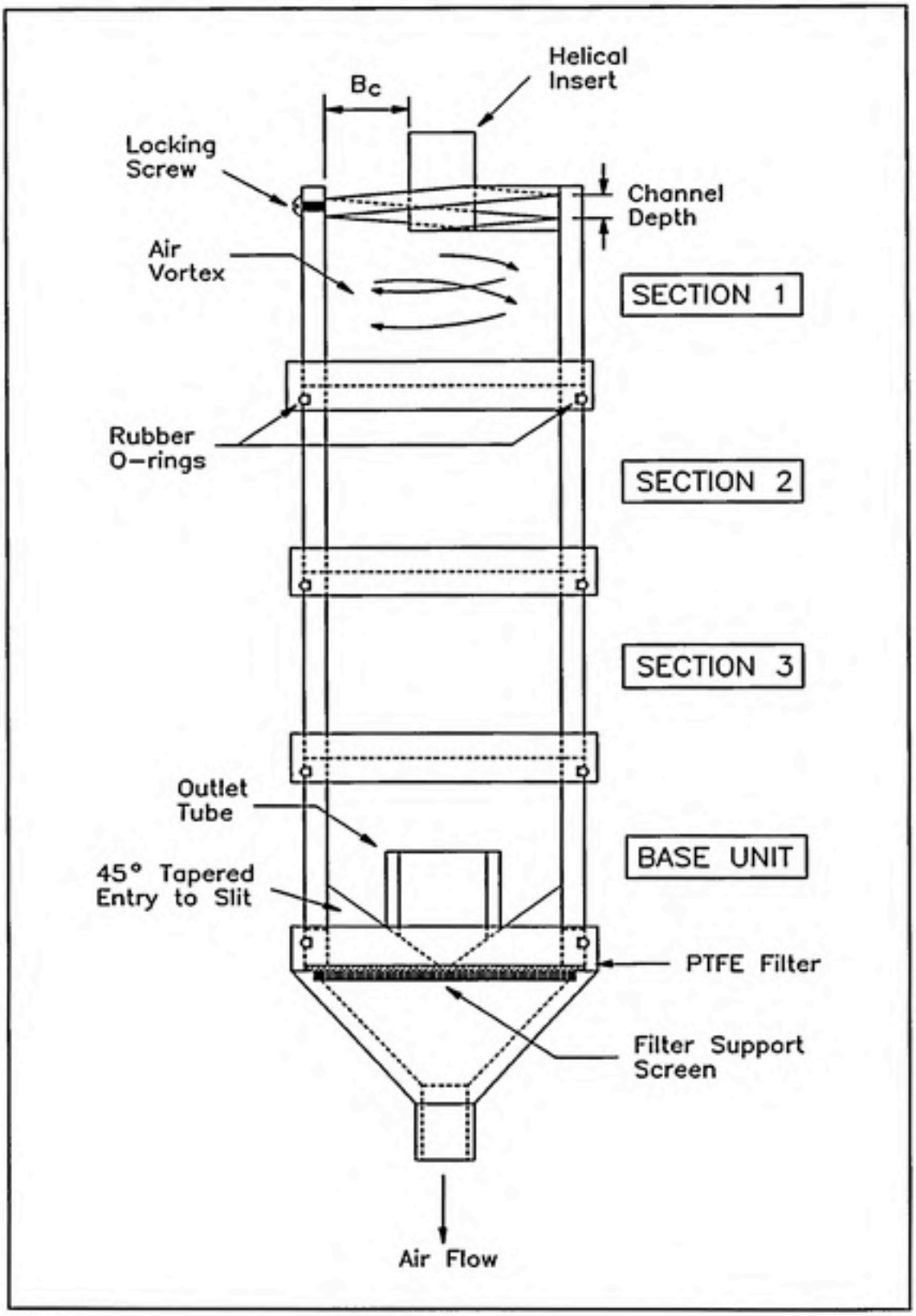

Figure 2.5: Labeled Schematic of Combined Cyclone Sections

Table 1.1: Cyclone Specifications

	DIMENSIONS centimeters (cm)
Cyclone Body	
Outside Diameter	5.0
Inside Diameter	4.1
Base Length	4.6
Coupling Length	4.1
Exit Slope	45°
Outlet Tube Diameter	2.5
Helical Insert	
Depth	1.0
Width 1	1.2
Width 2	1.5
Entry Angle	~5°
Slit	
Width	0.04
Length	4.0
Miscellaneous	
Distance from helix bottom to connector edge	2.0
Distance from outlet tube top to connector edge	1.8

III OBJECTIVES AND HYPOTHESIS

The primary objective of this project is the modification of the sampling inlet of the Mattson-Garvin slit-to-agar bioaerosol sampler to enable this sampler to provide data (particle size fractionation and concentration over time) on microorganism bearing particles in the ambient air. To accomplish this objective, determinant variables affecting the ability of the modified sampler to detect the general ambient aerosol concentration under specific conditions must be identified and evaluated. Some of the identified determinant variables may not be quantitatively amenable to evaluation, if at all. For example, temperature and humidity are measurable but not practically controllable variables. The dependent variables include:

Environmental Air (Direction and Speed of Air Movement) - relative vector of airstream motion of the ambient sampling atmosphere

Particle Size Distribution - frequency distribution of particle sizes in the ambient air stream

Temperature - degrees centigrade of the ambient air

Humidity - relative water content of air as determined by wet and dry bulb readings (psychrometer)

Surrounding Activity - natural occurrences (e.g., meteorological, radiant energy, etc.), human events, evolution of process by-products, etc., that effect the content, quality or other measurable parameters of the ambient air, and of which the sampling personnel have little or no control

Microbial Viability - capability of vegetative cell proliferation and the capacity to elicit competent biochemical responses of the given species

Sampler Sterility Between Samples - elimination of vegetative growth and spore-forming activity of microorganisms on critical surfaces by autoclaving or other sterilization techniques

Operator Sampling Technique - performance of sample collection, handling, storage, and analyses, according to standardized or accepted practices

Consideration of all the determinant variables (quantitatively and/or qualitatively) is instrumental in evaluating a working hypothesis of this

research project. However, a systematic evaluation of an individual determinant variable excluding the effects of the others can offer more insight into the sampling efficiency of the modified sampler. In particular, some these variables are not applicable to an evaluation of the sampling inlet at the exclusion of the sampler as a whole. The excluded variables include microbial viability, effective sampler sterility between samples, and, for practical purposes, temperature and humidity. A working hypothesis that summarizes the primary objective can be stated as:

> "The axial flow cyclone sampling inlet design is capable of efficiently fractionating particles into respirable and non-respirable size ranges (50% effective cut-off diameter at 8 μm). In addition, this modified sampling inlet is capable of collecting ambient aerosol particles as efficiently as the 47-mm filter cassette over a range of particle sizes under the same experimental conditions."

The hypothesis was tested for separation efficiency and sampling efficiency by performing independent comparisons of six cyclone configurations (varying helix inlet cross-sectional area and cyclone chamber length) to a reference sampler, the 47-mm filter cassette. The filter cassette, under "calm wind" conditions, has been shown to exhibit a sampling error of less than 20% for particles less that 15 μm in diameter [Fairfield, 1980]. Each of the six cyclone configurations were studied to determine the presence of

systematic differences or bias in the measured concentrations of aerosol sampled as a function of the separation efficiency on the cyclone filter and relative to the filter cassette (recovery efficiency). The null hypotheses to be tested are that (1) the separation efficiency mean is 50% at 8 μm and (2) the ratio mean between the cyclone and the reference sampler is 1 over a range of particle sizes.

IV CONDUCT OF EVALUATIVE EXPERIMENTS

The evaluation of each cyclone configuration was made under controlled experimental conditions to limit the effects of certain determinant variables to better comprehend the system operating characteristics. Using a horizontal aerosol chamber designed for the systematic evaluation of particulate air samplers, cyclone configurations were individually placed (side-by-side with a 47-mm filter cassette) in the interior downstream end of the chamber [Martinez, 1991; Jensen, 1991]. Monodisperse aerosol particles of oleic acid tagged with a fluorescent dye (uranine) were generated at the upstream end of the chamber using the Berglund-Liu vibrating orifice monodisperse aerosol generator (VOMAG). The TSI Aerodynamic Particle Sizer (APS) was used, at the sampler location, to verify particle size and aerosol generating system operation. The determinant variables investigated in this experimental study were particle size, helix entry cross-sectional area, and cyclone chamber length. All other variables were held constant (i.e. sampling stream air velocity, and sampler angle to the sampling stream). Temperature and humidity were assumed to remain constant.

4.1 EXPERIMENTAL EQUIPMENT

4.1.1 Aerosol Chamber

Vertical laminar flow aerosol test chambers have been described in the literature for evaluation and calibration of sampling instruments [Marple and Rubow, 1983; Hinds and Kraske, 1987]. However, the aerosol chamber to be used in this study was designed with a horizontal axis similar to the American Society of Heating, Refrigeration, and Air-conditioning Engineers (ASHRAE) air cleaner standard test duct [ASHRAE Handbook, 1983]. The chamber is composed of a stainless steel duct of approximately 366 cm in length and having a square cross-section of 61 cm in length on each side (a schematic diagram is shown in Figure 4.1). High efficiency particulate air (HEPA) filters were placed at the inlet and outlet of the chamber to provide an uncontaminated flow of air to the samplers. Two baffles were after the point of aerosol introduction to provide a uniform particle concentration across the cross-sectional face of the chamber. Access to the chamber interior was facilitated through a plexi-glass observation window held in place with clamps. The aerosol chamber was designed to give an air velocity at the point of the sampler challenge test of approximately 25 to 50 centimeters per second (cm/sec) resulting in a volumetric flow rate of 340 to 680 cubic meters per hour (m^3/hr) of air. For a flow rate of 340 m^3/hr the resultant air velocity, obtained by conducting horizontal and vertical traverse with a thermoanemometer (KURZ 1440, Kurz Instruments, Inc., Monterey, CA), was 26 $\pm$ 1 cm/sec and a flow rate of 680 m^3/hr resulted in an air

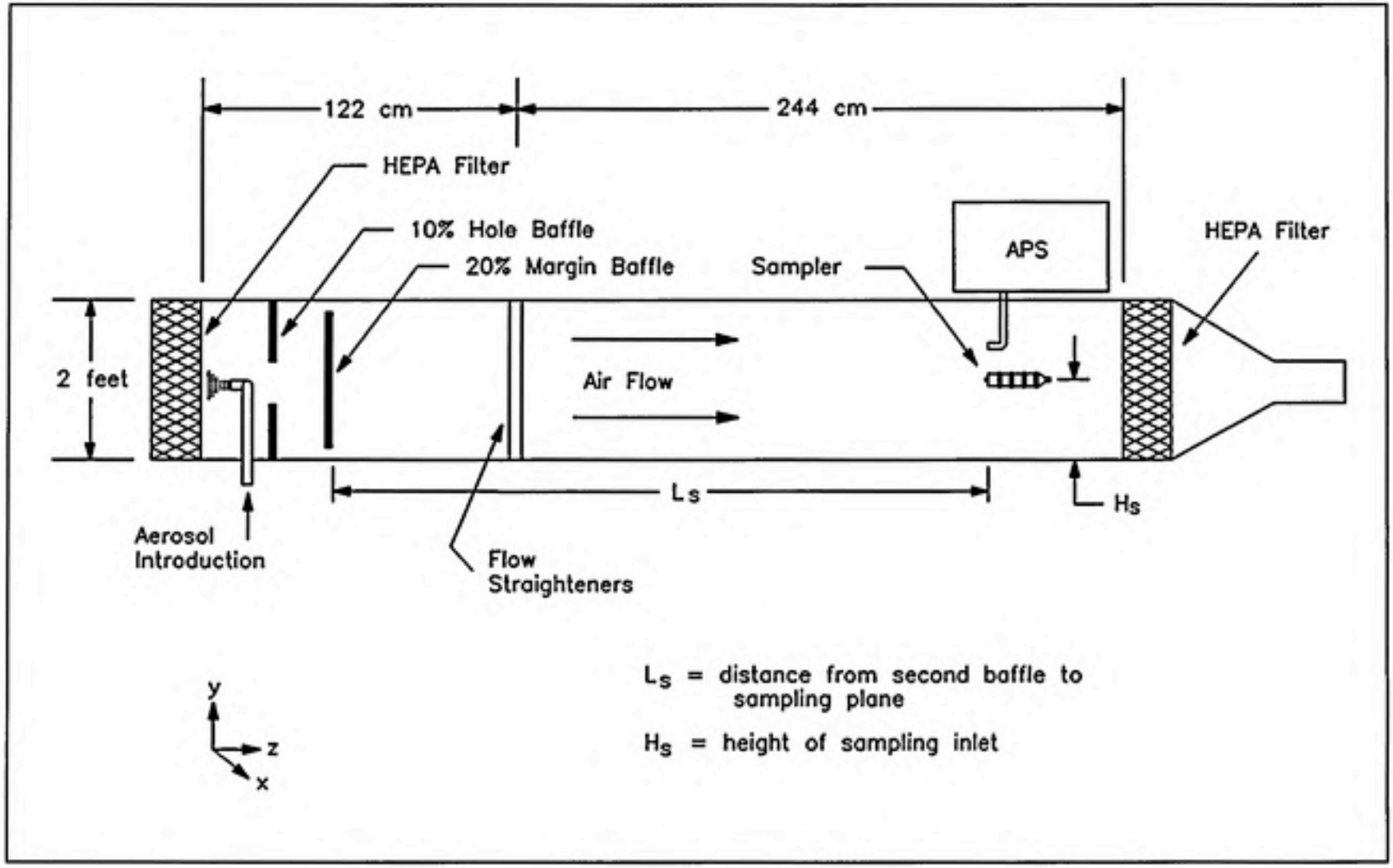

Figure 4.1: Schematic of Aerosol Chamber

velocity of 57 ± 1 cm/sec. This low velocity falls within the still-air sampling criteria (reminiscent of real-world conditions) as defined by the following equation [Hinds, 1982]:

$$U_0 \leq \frac{1}{5}\left(\frac{Q}{4\pi\tau^2}\right)^{1/3} \qquad (6)$$

where U_o is the maximum air velocity for which the still-air sampling criteria can be used, Q is the sampler flow rate in cm^3/sec, and τ is the particle relaxation time for a given diameter [Hinds, 1982]. For 10 μm diameter particles (unit density spheres) at a sampler flow rate of 28 lpm, the maximum allowable air velocity to meet the criteria is approximately 145 cm/sec.

Elutriation, which is an inevitable consequence of the decay of an aerosol particle trajectory along the critical path of a horizontal duct, should not be a problem for the particle size ranges to be encountered in this study. The height (H) that a particle will settle over the chamber length from the last baffle plate to the sampler inlet location (L_s) is given by the following equation:

$$H = \frac{L_s V_{ts}}{V_{chamber}} \qquad (7)$$

where V_{ts} is the terminal settling velocity at a given particle size and $V_{chamber}$ is the air velocity in the chamber, both in cm/sec. Based on this equation, a

particle with a diameter of 10 μm will settle 2.8 cm from the last baffle plate to the sampler inlet. The Reynolds number (*Re*) associated with flow of air inside the chamber is governed by the following equation [Reist, 1984]:

$$Re = \frac{\rho w V_{chamber}}{\mu} \qquad (8)$$

where *w* is the chamber width is feet, ρ is the density of the air, and μ is the viscosity of the air. For a chamber air velocity of 25 cm/sec (flow rate of 340 m^3/hr), the *Re* is in the turbulent regime (10,200, where greater than 4000 is turbulent).

Horizontal and vertical chamber traverses were conducted in the sample plane using an Aerodynamic Particle Sizer (a narrative of the instrument operation can be found in section 4.1.3) which provided real-time detection of aerodynamic particle size and particle concentration. The resultant data from the traverses are graphically presented in Figures 4.2 and 4.3. The mass median aerodynamic diameter (MMAD) for horizontal and vertical traverses for the aerosol chamber design were measured to be 5.37 μm $\pm$ 0.08 μm and the mass concentration was measured to be 0.22 $\pm$ 0.01 particles/cm^3.

4.1.2 Aerosol Generation

A Berglund-Liu vibrating orifice monodisperse aerosol generator was used to produce aerosol particles of fluorescently tagged (with uranine) oleic acid

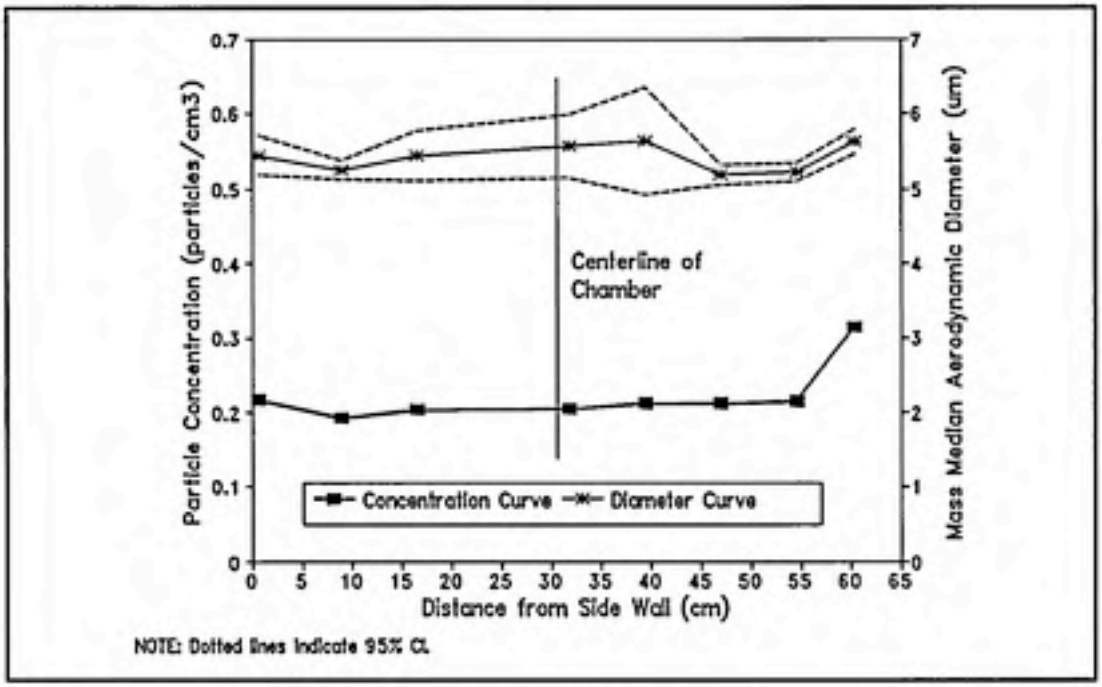

Figure 4.2: Aerosol Chamber Particle Concentration and MMAD - Horizontal Traverse in the Sampler Plane

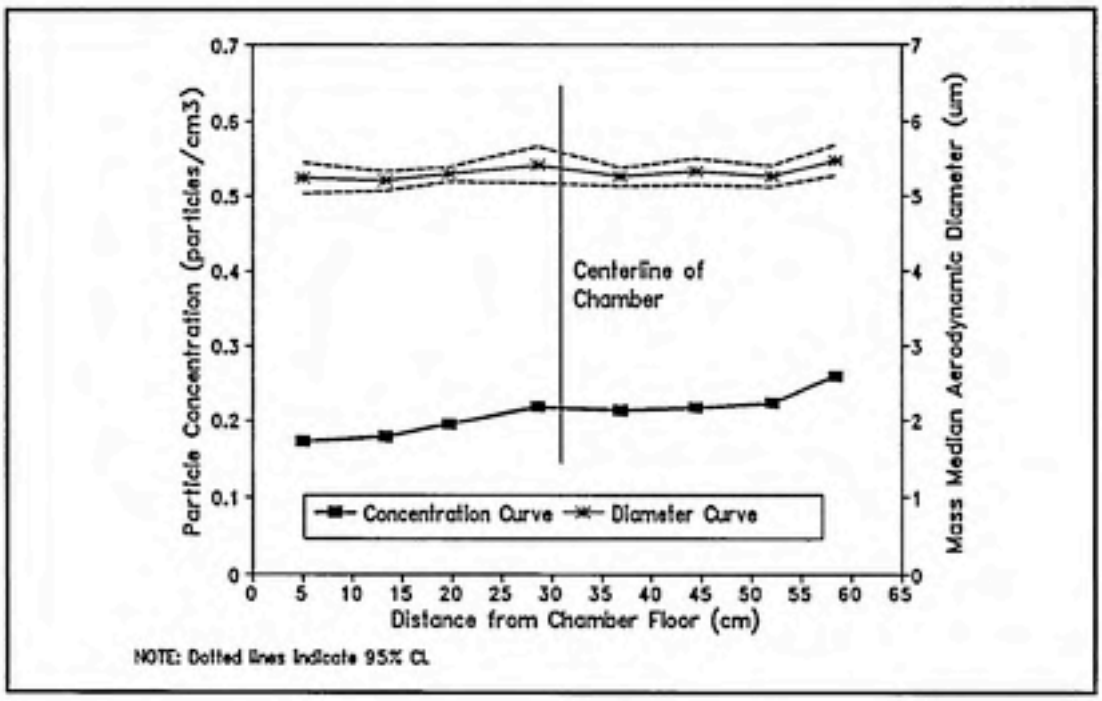

Figure 4.3: Aerosol Chamber Particle Concentration and MMAD - Vertical Traverse in the Sampler Plane

with a nominal aerodynamic diameters of 3, 4.5, 6, 8, 10 μm [Berglund and Liu, 1973; Willike, 1975]. The VOMAG operates through the combined contributions of four parts: the liquid feed system, the droplet generator, the droplet dispersion system, and the aerosol flow system (Figure 4.4). The liquid feed system forces a liquid (consisting of a mixture of alcohol, oleic acid, and uranine) through a membrane filter into the droplet generator at a constant rate. For this study, a 50 cubic centimeter (cm^3) syringe was pressurized with desiccated, filtered air, which provides a stable feed rate to the droplet generator. The calibration curve relating pressure (kiloPascals - kPa) and liquid feed rate (cubic centimeters per minute - cm^3/min) is shown in Figure 4.5. The droplet generator houses a 20 μm orifice disc through which the liquid flows. An AC voltage is applied to the piezoelectric ceramic which vibrates the disc and disturbs the liquid jet at a constant (selectable) frequency. The dispersion air from the droplet dispersion system creates a turbulent air stream which forces the enveloped droplet stream into a dispersed conical shape. The aerosol flow system uniformly disperses the droplets and allows the alcohol to volatilize leaving individual droplets of a specific, predetermined size. From Berglund and Liu, the size of the individual particles (D_p) can be computed from the following formula:

$$D_p = C^{1/3} \left(\frac{6 Q_l}{\pi f} \right)^{1/3} \qquad (9)$$

where Q_l is the liquid feed rate in cubic centimeters per minute, f is the vibration frequency of the piezoelectric ceramic in Hertz, and C is the

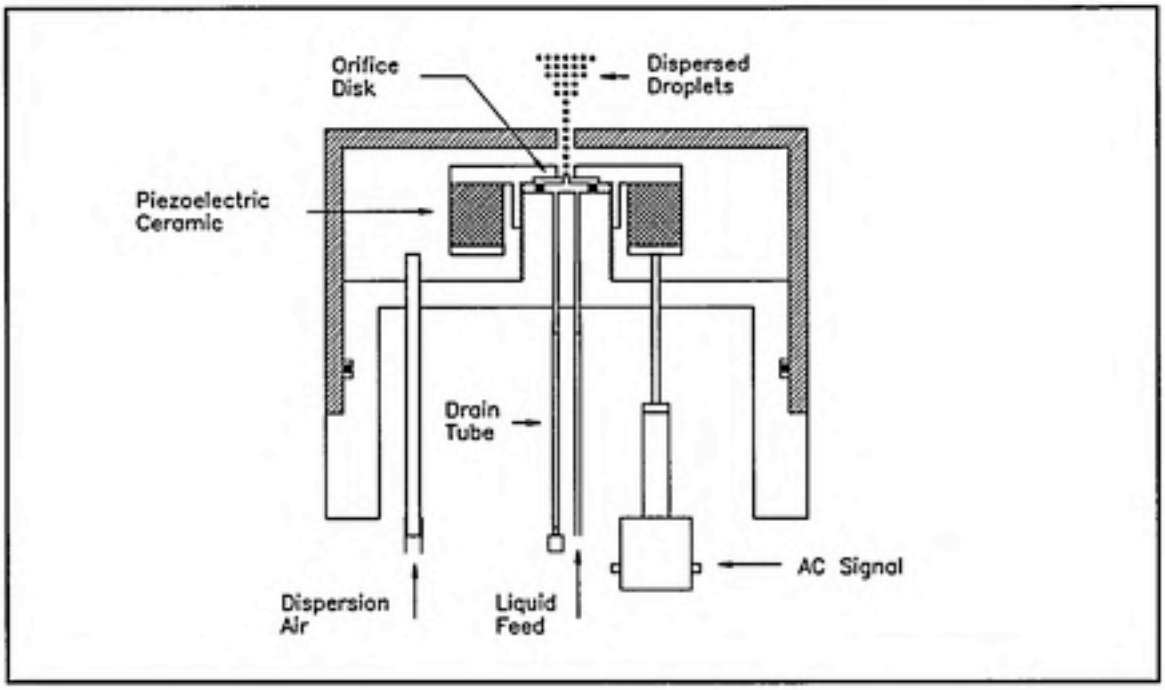

Figure 4.4: Schematic of Berglund-Liu Vibrating Orifice Monodisperse Aerosol Generator

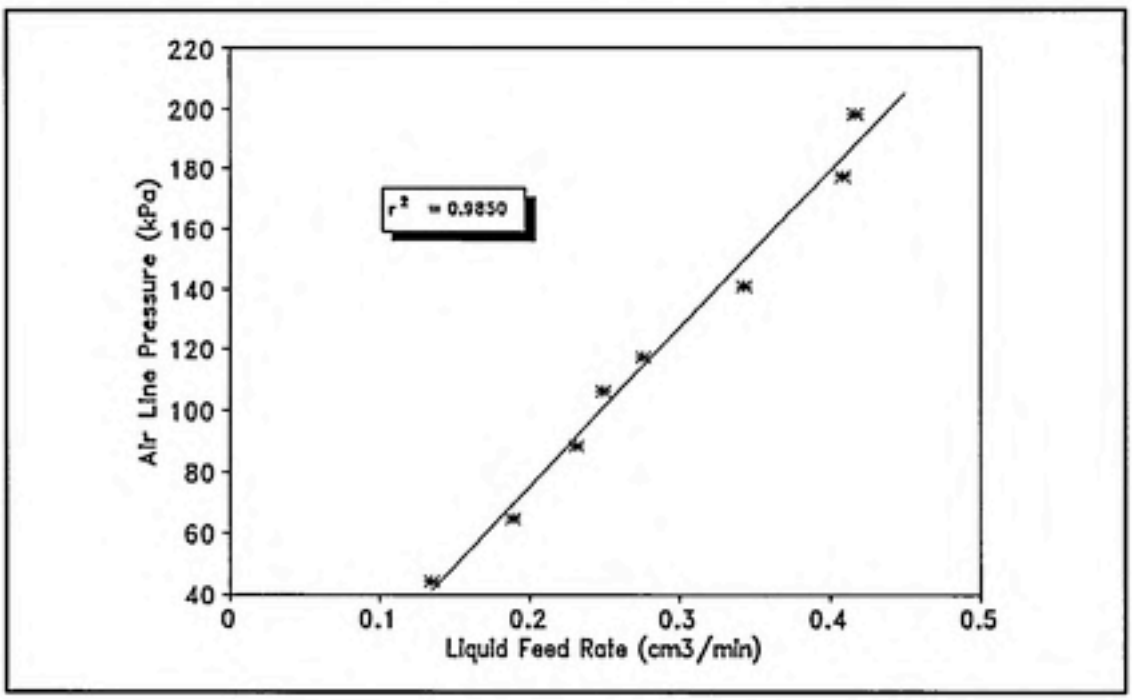

Figure 4.5: Calibration Curve for VOMAG Liquid Feed System

concentration of the nonvolatile solute dissolved in the volatile solvent. The diameters of particles generated by the VOMAG can be calculated, from the above equation, to less than a 1% error from the generator operating conditions. The stability of the generated aerosol has been determined to have a variation in concentration less than 3% [Berglund, 1972]. Due to the importance of keeping the orifice disc clear of particulate matter, all reagents used in this investigation were of spectroscopic grade and solutions underwent series filtration through two 0.45 μm pore size membrane filter. However, some particulate matter remained suspended in solution as determined by generation of aerosol particles of filtered alcohol and subsequent particle size analysis with the APS. Treating the addition of uranine as an impurity, the aerodynamic diameter (D_a) can be computed from:

$$D_a = ((C+I+U)D_p)^{1/3}\sqrt{\rho_{avg}} \qquad (10)$$

where C is the volumetric concentration of oleic acid in alcohol, I is the concentration of impurities in the alcohol, U is the concentration of uranine in solution, and ρ_{avg} is the average density of the oleic acid and uranine.

A series of static eliminators was placed around the base of the dilution column (approximately 5.1 cm above the point of aerosolization) to neutralize the charge of the aerosol particles before entering the chamber. The aerosol was introduced from the side of the chamber approximately 1.5

cm short of centerline to account for the momentum of the particles in the lateral direction (i.e. perpendicular to the flow of oncoming chamber air).

4.1.3 Verification of Aerodynamic Diameter

Real-time detection of the aerodynamic particle size and particle concentration in the aerosol chamber were conducted in the sample plane using an Aerodynamic Particle Sizer (APS 33B, TSI, Inc. Minneapolis, MN). The APS accelerates aerosol particles through a nozzle which then pass through a laser velocimeter (Figure 4.6) [Chen et al., 1985; Ananth and Wilson, 1988; Griffiths et al., 1986]. The inertia of the particles causes the particles to lag behind the downstream air from the nozzle. The extent of the lag between the particle velocity and the gas velocity is based on the aerodynamic diameter of the particle. The APS was originally calibrated with Polystyrene Latex spheres (solid particles), therefore the effect of liquid droplet deformation in the sample air stream will indicate particle diameters smaller than that predicted by the VOMAG [Baron, 1986]. However, the droplet deformation would not affect the particle count. The duration of each APS sampling period was 10 minutes.

4.1.4 Sample Analysis

Fluorometric analysis is very sensitive (which was a necessity for the dilute solutions encountered in this experiment). The method also lends itself to simplicity and specificity. Since there is a linear relationship between

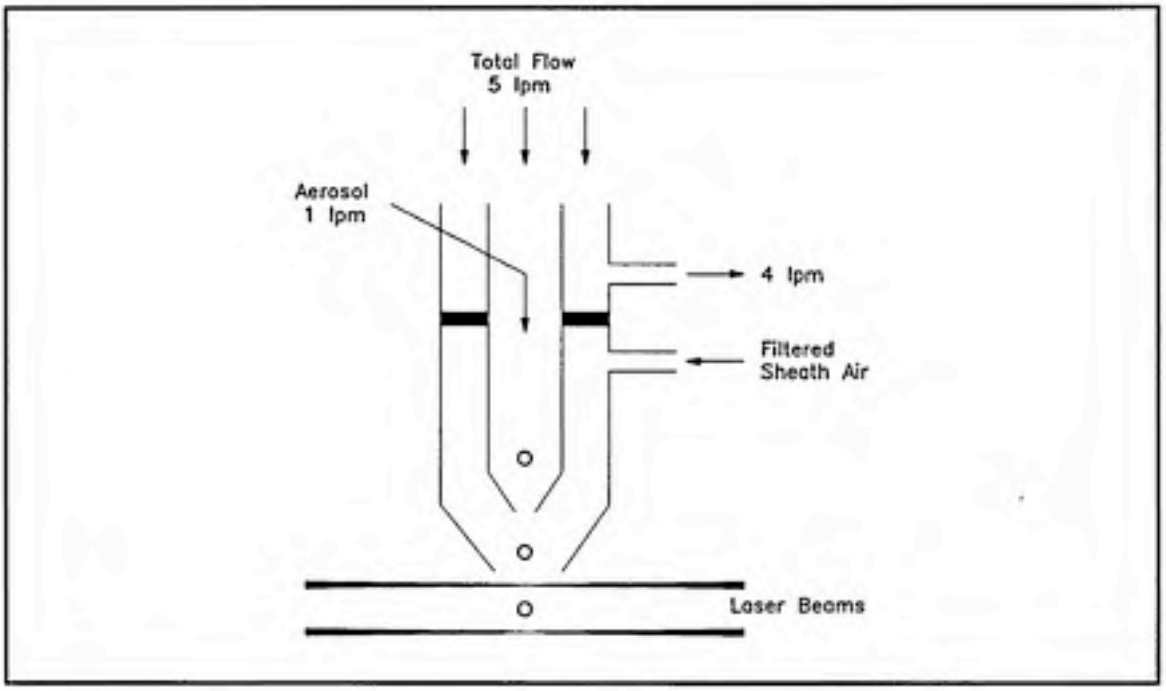

Figure 4.6: Schematic of TSI Aerodynamic Particle Sizer

concentration and fluorescence, it is possible to construct a calibration curve based on a standard. During the process of aerosolization from the VOMAG, the alcohol volatilizes leaving fluorescently tagged oleic acid particles. These particles can then be quantified in solution based on the resultant fluorescence produced. The method is pH sensitive (optimal pH is approximately 10). A Perkin-Elmer fluorescence spectrophotometer (Model 650-10S) was used to quantify the amount of aerosol that had been collected by the cyclone and 47-mm filter cassette. This instrument is specifically designed for the measurement fluorescence excitation and emission spectra. The light source is a 150-watt xenon lamp. Both grating monochromators have continuously variable bandpass selection from 1.5 to

20 nanometers (nm). The sample is irradiated by the light from the excitation monochromator in the 220 to 830 nm wavelength range. The emitted light from the sample passes through the emission monochromator (selective measurement of intensity is 220 to 820 nm) to a photomultiplier detector [Perkin-Elmer, 1978].

The relationship between fluorescence intensity and concentration has been well described [Underfriend, 1962; Hercules, 1966; Guilbault, 1973]:

$$(S_f)_\lambda = f(\theta)\, g(\lambda)\, I_0 \phi_f abc \left[1 - \frac{abc}{2!} + \frac{\overline{abc}^2}{3!} - \cdots + \frac{\overline{abc}^n}{(n+1)!}\right] \qquad (11)$$

where $(S_f)_\lambda$ is the sample fluorescence intensity at a given wavelength, $f(\theta)$ is the geometry depending on the effective solid angle, $g(\lambda)$ is the response characteristic of the detector (varies with wavelength), I_0 is the intensity of the exciting radiation, ϕ_f is the quantum efficiency of the molecule, a is the molar absorptivity for the sample at the exciting wavelength, b is the sample path length along the axis of irradiation, and c, is the concentration of the fluorescing material in moles per liter. In situations, as were encountered in this study, where the concentration of fluorescing material is very small ($abc < 0.05$) the equation reduces to:

$$(S_f)_\lambda = f(\theta)\, g(\lambda)\, I_0 \phi_f abc \qquad (12)$$

Spectral scans were conducted on a 0.2 microgram per milliliter (μg/ml)

solution of uranine in 0.01 N Sodium Hydroxide (NaOH) to determine the optimum excitation and emission wavelengths (shown graphically in Figure 4.7). Calibration curves, for the low and normal photomultiplier tube gain, were then developed using a stock solution of 20 μg/ml uranine and 0.01 N NaOH. This solution was added to 0.01 N NaOH to produce sequential dilutions of 0.1, 0.05, 0.01, 0.005, 0.001, 0.0005, and 0.0001 μg/ml. The resultant calibration curve is shown in Figure 4.8.

For the analysis of the filter samples, the fluorescence spectrophotometer slit widths were set at 5 and 10 nm for the excitation and emission wavelengths, respectively. The narrower excitation slit width was selected to guard against photo-chemical reactivity of the sample solutions. The excitation wavelength was reduced to 484 nm, which is below the optimum wavelength of 492 nm as determined by the spectral scan. The reduction of the excitation wavelength and the narrower excitation band pass promoted the minimization of interference of Rayleigh scatter peaks with emission peaks due to the close proximity of the excitation and emission peaks [Perkin-Elmer, 1978]. The optimum emission wavelength of 512 nm was used for all analyses.

The 47-mm, 2 μm polytetrafluoroethylene (PTFE or Teflon®, Gelman Sciences, Ann Arbor, Michigan) filter from each cyclone experimental run was divided into three sections using a scalpel. The divisions between the

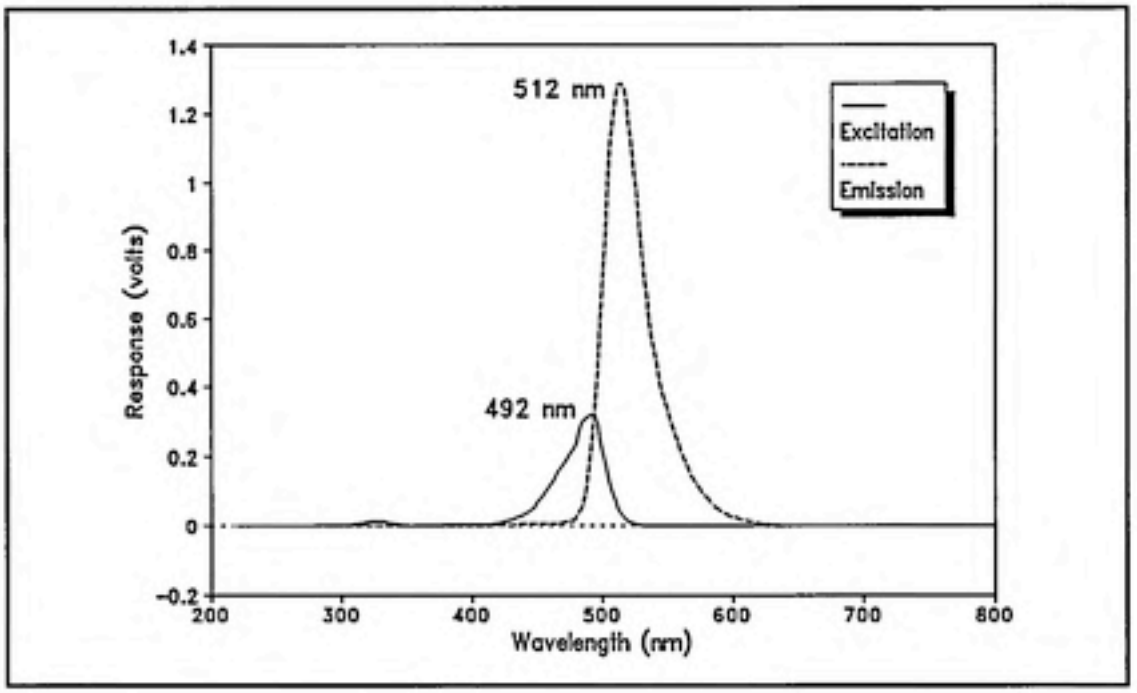

Figure 4.7: Excitation and Emission Spectrums for a 0.2 μg/ml Solution of Uranine in 0.01 N NaOH

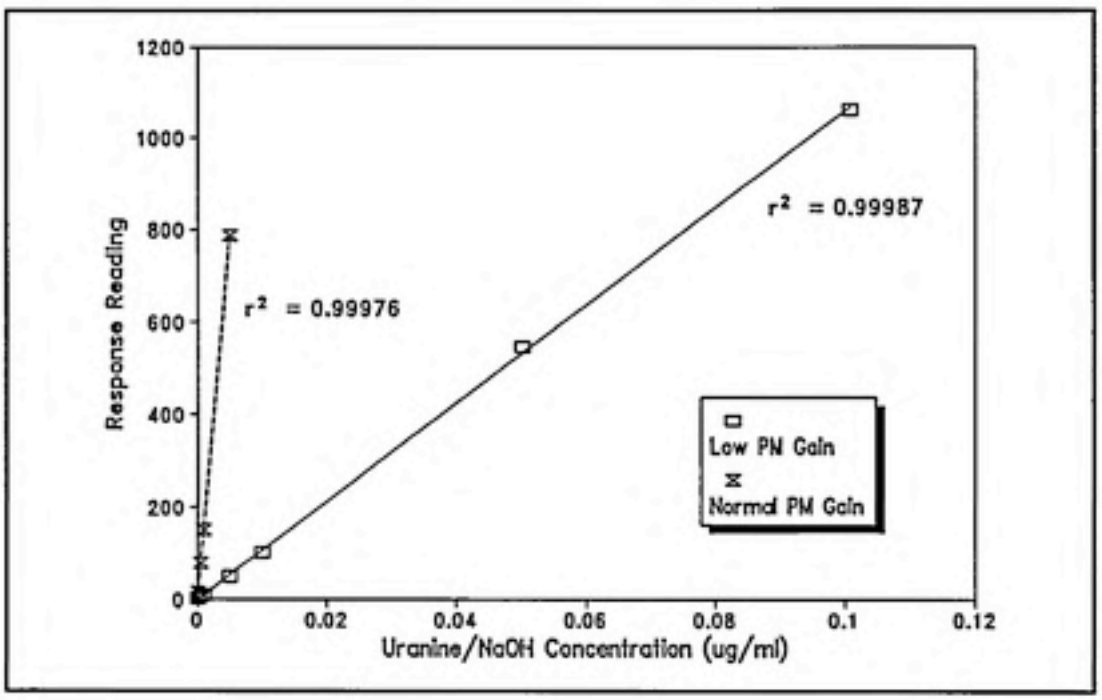

Figure 4.8: Calibration Curves

two outer sections and the inner section are represented by two tangentially intersecting lines at the diameter of the cyclone exit tube. The outer and inner sections were separately placed in two separate glass jars for later analysis. The filters from the cyclone or the filter cassette were placed face down in each jar. For the cyclone sample, 15 ml of 0.01 N NaOH was added to each outer and inner section jar. For the filter cassette sample, 30 ml of 0.01 N NaOH was added to each jar. The samples were then placed in an ultrasonic bath for 30 minutes. Analysis in the fluorescence spectrophotometer was facilitated by placing approximately a 4 ml aliquot of the sample solution into a cuvette. Response readings from the digital display were converted to units of $\mu g/m^3$ of air based on the calibration curve. The selection of the filter media, wash-off solution, and analytical technique were based on the results of Tseng [Tseng, 1991]. Tseng conducted experiments evaluating the effects of two filter medias (glass fiber and PTFE filters) and various wash-off solutions (H_2O with and without a buffer, 0.001, 0.01, and 0.1 N NaOH solutions, and ethanol with and without a buffer). Tseng found (1) no background reading from PTFE filters, (2) 0.01 N NaOH is a suitable solvent for PTFE filters based on its high extraction ability and non-existent background reading, and (3) 30 minutes in an ultrasonic bath effectively removes all the uranine from the filter. All sample aliquots were analyzed twice. Blanks, for the cyclone and the filter cassette, were obtained at the conclusion of each days sampling run and subtracted from each individual series result.

4.2 EXPERIMENTAL DESIGN

Preliminary investigation of the operating characteristics of the modified sampling inlet revealed shortcomings related to its sampling efficiency. At a VOMAG generated particle size of 12 μm, tandem sampling runs with a single cyclone configuration and the 47-mm filter cassette resulted in sampling efficiency of less than 0.05% and separation efficiencies inconsistent with the design aspects of the cyclone. Based on these observations, a series of experiments were initiated to investigate the effect of various cyclone flow rates to improve the sampling efficiency of the system. Experiments to evaluate the effect of cyclone configurations on the separation efficiency were then conducted after the determination of an optimum flow rate.

Each sampler (i.e. cyclone, 47-mm filter cassette, and APS) was oriented in the chamber so that the midline of the sampler is facing the aerosol generator output source at a predetermined reference point. This particular sampler orientation resulted in isoaxial sampling. The criteria of isokinetic sampling are not applicable here due to the still-air sampling assumption. All sampling devices were located 276.9 cm downstream of the second chamber baffle (refer to Figure 4.1). The cyclone and filter cassette were placed at a height of 30.5 cm above the chamber floor in the vertical plane. In the horizontal plane, the cyclone and the filter cassette were positioned 11.4 cm on either side of the chamber centerline. The APS probe was

located 43.2 cm above the chamber floor and 12.7 cm from the chamber wall to the right of the cyclone. The 47-mm filter cassette and the APS were operated at flow rates of 14 and 5 lpm, respectively. The filter cassette was fitted with a 2.5 cm diameter cone to provide a "sharp-edged orifice" entry.

A rotameter (Cole-Parmer, Chicago, Illinois) was placed in-line between each sampler (i.e. cyclone and 47-mm filter cassette) and rotary pump (used to pull the required volumetric flow of air). The cyclone and the 47-mm filter cassette were calibrated over a range of flow rates, from 0.9 to 34.3 lpm, using a 150 liter spirometer. All calibration measurements were made with the PTFE filters inserted into the appropriate sampling device. Desired adjustments to the sampler flow rate during experimental runs were made based on the rotameter calibration curve. The calibration curves are shown in Figure 4.9.

4.2.1 Variable Flow Rate Experimental Design

A single cyclone configuration (wide helix cross-sectional inlet area and medium cyclone body length) was used to evaluate the effect of varying flow rates on the collection efficiency of the system. Each experimental run (one cyclone configuration) was conducted in tandem with the 47-mm filter cassette and the APS over a 15 minute sampling period. Six experimental conditions were studied by varying particle size at levels of 3.5, 9.4, and

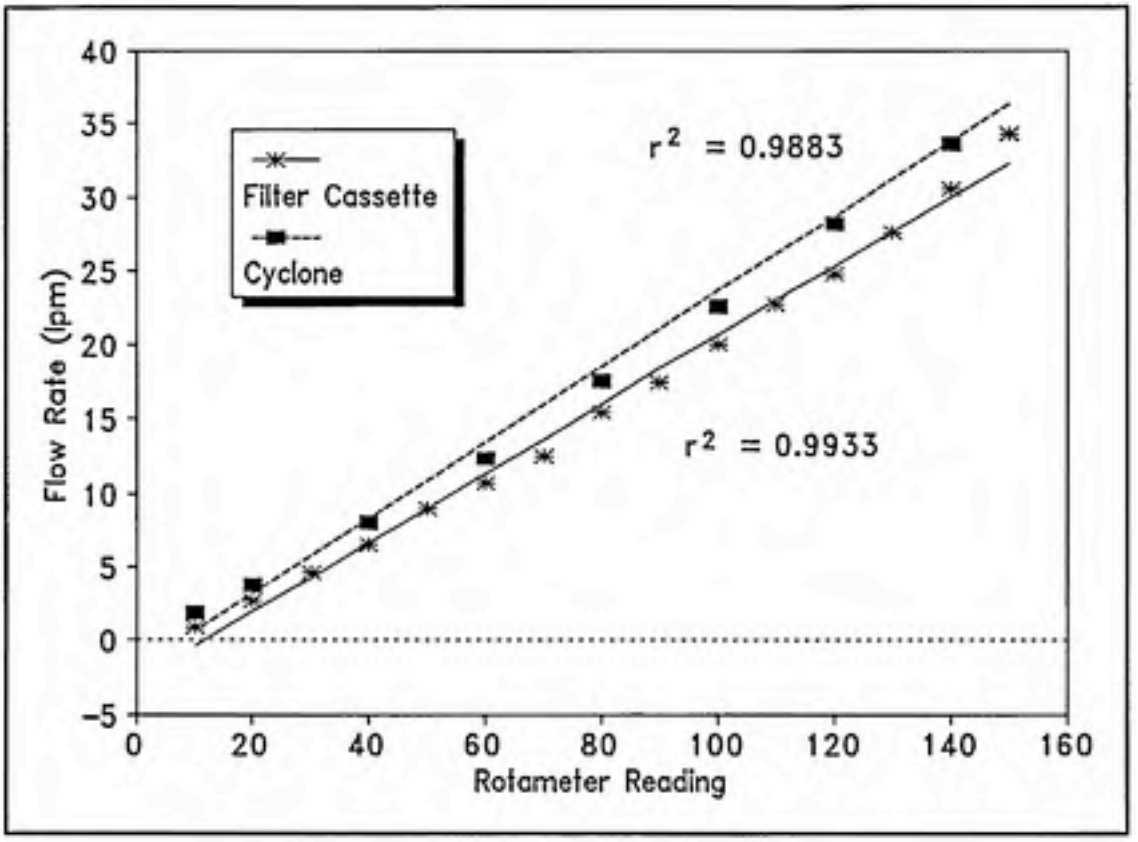

Figure 4.9: Calibration Curves for In-line Rotameters

14.1 μm and by varying cyclone flow rate at levels of 7, 14, and 28 lpm. Experimental study blocks were designated over a full day with all flow rates being evaluated three times at a specific particle size on any given day. The sequence order for flow rates within a given day were randomly allocated. In addition, particle size was randomly selected over successive days of experimental sampling. The experimental design allowed 6 repetitions at a specific flow rate and particle size.

4.2.2 Various Cyclone Configurations Experimental Design

From the flow rate study a flow rate was selected (7 lpm) that optimized the

collection efficiency of the cyclone. Each experimental run was conducted in tandem with the 47-mm filter cassette and the APS for a 15 minute sampling period. Thirty experimental conditions were studied by varying helix cross-sectional inlet area at two levels, clone body length at three levels, and particle size at levels of 3.6, 5.3, 7, 9.3, and 11.8 μm. Experimental study blocks were designated over a full day with all cyclone configurations being evaluated twice on any given day. The sequence order for cyclone configuration within a given day were randomly allocated. In addition, particle size was randomly selected over successive days of experimental sampling. The experimental design allowed 4 repetitions of a specific cyclone configuration and particle size.

V RESULTS AND DISCUSSION

5.1 Variable Flow Rate Experiment

The summary results of the experimental runs evaluating the effect of different sampler flow rates on sampling efficiency is presented in tabular format in Table 5.1 and graphically in Figure 5.1. The individual results are presented in the appendix.

Table 5.1: Summary Results of Variable Flow Rate Experiment

Aerodynamic Particle Size (μm)	Flow Rate (lpm)	Sampling Efficiency	
		Mean	Standard Deviation
3.5	7	60.2%	7.3%
	14	54.3%	2.8%
	28	28.8%	1.4%
9.4	7	43.3%	2.6%
	14	6.3%	0.7%
	28	<0.1%	<0.1%
14.1	7	10.4%	2.0%
	14	<0.1%	<0.1%
	28	<0.1%	<0.1%

To facilitate statistical analysis, the concentration for the cyclone was divided by the paired measurement from the 47-mm filter cassette to calculate the variable SAMPEFF (corresponding to the sampling efficiency of

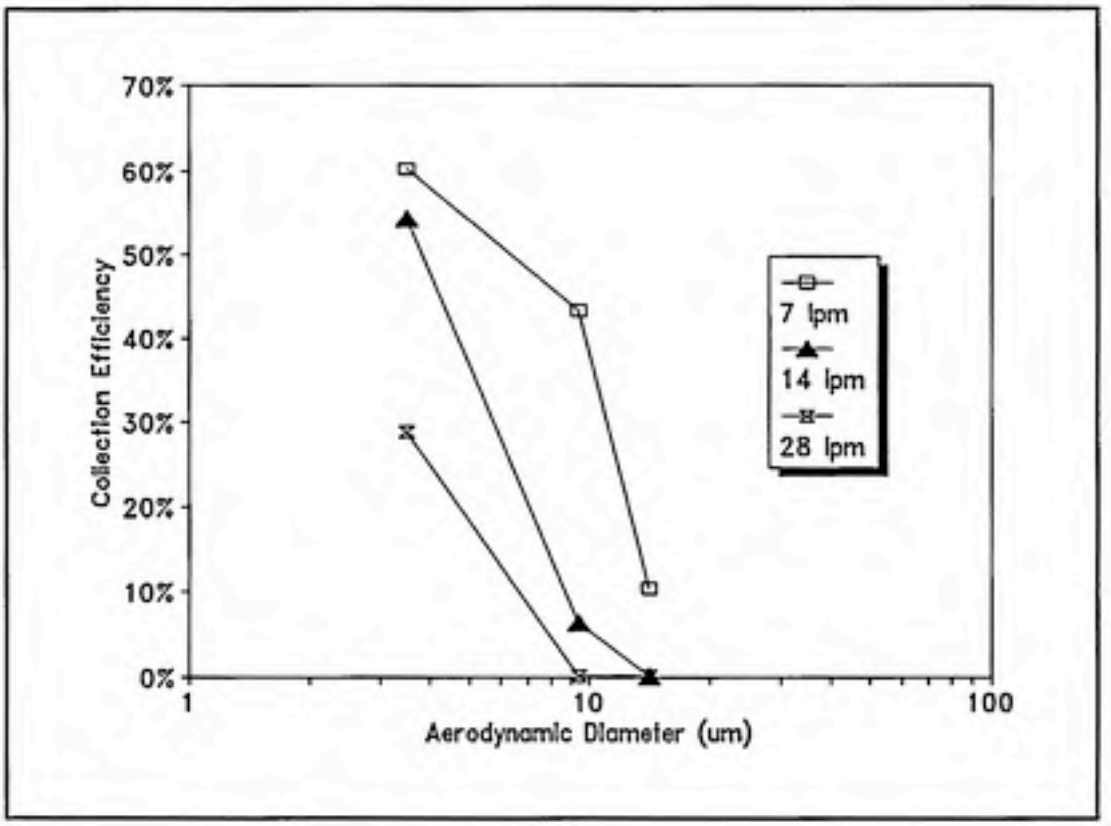

Figure 5.1: Graphical Results of Variable Flow Rate Experiment

the system). A separate variable, SAMPEFF0, was subsequently created by subtracting the value 1 from SAMPEFF. Complete agreement in measured levels between the cyclone and the filter cassette would imply that all differences are from a population with a mean of zero (the cyclone and the filter cassette obtain the same concentrations of the sampled air or SAMPEFF0 = 0). Agreement, except for a stable or consistent bias, would imply the same result but the mean of the response variable would be non-zero. Systematic differences in measurements (bias due to flow rate and/or particle size) would imply at least two populations with different means.

A two-way Analysis of Variance (ANOVA) was used to determine the agreement between the cyclone and the filter cassette using the response variable SAMPEFF0. First, the null hypothesis of no overall bias is tested by reference to the F-ratio for all effects in the model, i.e. the flow rate effect, the particle size effect, and the intercept. Lack of significance at the 0.05 level indicates no statistical difference of the population means. No further statistical testing is conducted in this case. A significant F-ratio indicates the presence of some bias. If this test indicates the presence of a bias, it could be a consistent bias of the same magnitude for all flow rates and particle sizes or that the level of bias varies among the three flow rates and/or three particle sizes. A significant flow rate and/or particle size indicates the latter condition. If particle size is not significant, it is meaningful to test for a consistent bias by testing that the grand mean, intercept, is zero.

The results from the statistical analyses indicate that the overall bias was significant ($p<0.001$) and the variation of bias by flow rate and/or particle size was significant ($p<0.001$). The mean bias was negative, at the 0.05 significance level ($p<0.001$), indicating that the cyclone underestimates the filter cassette. In addition, a significant bias ($p<0.001$) was detected for the interaction between flow rate and particle size.

Statistically, it is evident that a reduction of the cyclone flow rate from the

designed value (28 lpm) can improve the sampling efficiency of the system. These results gain further validity upon observation of the helical insert. A deposit of uranine was visible below the entry lip to the helix at the higher flow rates and larger particle sizes. The entry to the helix may act as an impaction device, whereupon larger particles cannot make the high velocity turn from the ambient air stream into the vortex of the cyclone. The entry lip deposit was not as pronounced or non-existent for the low flow rate (7 lpm) and the smallest particle size investigated (3.5 μm). Based on these analyses and observations, the flow rate of the cyclone was reduced to 7 lpm for the investigation of the various cyclone configurations. It was suspected, prior to the initiation of the cyclone configuration study, that a reduction of the cyclone flow rate would shift the separation efficiency curve to the right, effectively increasing the value of the 50% cut-off diameter. Even at this reduced flow rate of 7 lpm, the cyclone system will under-estimate the concentration inside the chamber as compared to the filter cassette based on the results of the flow rate study. However, the continued evaluation of the system will reveal the cyclones ability to function as designed, i.e. aerosols will move to the walls of the cyclone, hence, be separated into two zones of collection on the filter based on the particle aerodynamic diameter.

5.2 Various Cyclone Configurations

The summary results of the experimental runs evaluating the effect of

various cyclone configurations on separation efficiency and recovery efficiency is presented in tabular format in Table 5.2 and graphically in Figures 5.2, 5.4, 5.6, and 5.7. The separation efficiency calculated on an equal area basis (termed percent enrichment) is graphically presented in Figures 5.3 and 5.5. The general trends between sampling efficiency and percent enrichment remain consistent, however, percent enrichment indicates higher values. The higher values are the result of a smaller area on the outer filter zone available for particulate collection. The use of separation efficiency or percent enrichment for the statistical analyses will not affect the conclusions. The term recovery efficiency is used in place of sampling efficiency because this experiment includes the separation of the cyclone filter. The physical division of the filter may reduce the apparent sampling efficiency of the system. The individual results are presented in the appendix.

5.2.1 Statistical Analyses of the Cyclone Separation Efficiency

The statistical analyses used to assess the effect of the various cyclone configurations on the separation efficiency of the system were very similar to those used in the variable flow rate experiment. The particle concentration in the outer zone of the cyclone filter was divided by the particle concentration on the entire filter to create a variable SEPEFF (corresponding to the separation efficiency of the system). Systematic differences in measurements (bias due to helix design, cyclone tube length,

Table 5.2: Summary Results of Various Cyclone Configurations

Helix Design	Cyclone Tube Length	Aerodynamic Particle Size (μm)	Separation Efficiency		Recovery Efficiency	
			Mean	STD	Mean	STD
Thin	Short	3.6	15.5	2.4	54.8	2.1
		5.3	21.1	6.5	74.6	9.6
		7	29.7	16.1	54.9	5.3
		9.3	31.0	3.3	32.0	6.8
		11.8	33.3	7.6	15.9	1.1
	Medium	3.6	18.4	4.5	59	1.4
		5.3	19.9	8.3	67.4	15.2
		7	29.6	9.0	56.5	3.1
		9.3	23.0	3.2	31.9	8.0
		11.8	27.7	5.0	16.3	4.4
	Long	3.6	15.5	1.9	54.5	5.7
		5.3	16.4	10.4	68.9	15.7
		7	20.8	3.1	57.6	4.4
		9.3	21.1	5.3	32.5	6.0
		11.8	23.9	5.4	16.5	2.0
Wide	Short	3.6	16.0	1.1	60.2	4.9
		5.3	17	7.2	63.9	7.3
		7	29.2	9.8	65.8	6.4
		9.3	26.2	1.5	46.9	6.0
		11.8	32.5	2.9	32.7	1.7
	Medium	3.6	21.2	6.2	65.1	3.6
		5.3	22.0	13.3	64.4	26.8
		7	23.9	7.4	58	8.7
		9.3	24.4	2.3	44.8	3.4
		11.8	20.7	5.0	35.9	4.1
	Long	3.6	15.9	2.7	57.1	3.3
		5.3	13.8	7.6	69.8	12.1
		7	22.1	7.4	61.0	2.6
		9.3	23.0	4.9	47.0	3.6
		11.8	26.8	5.2	35.5	3.9

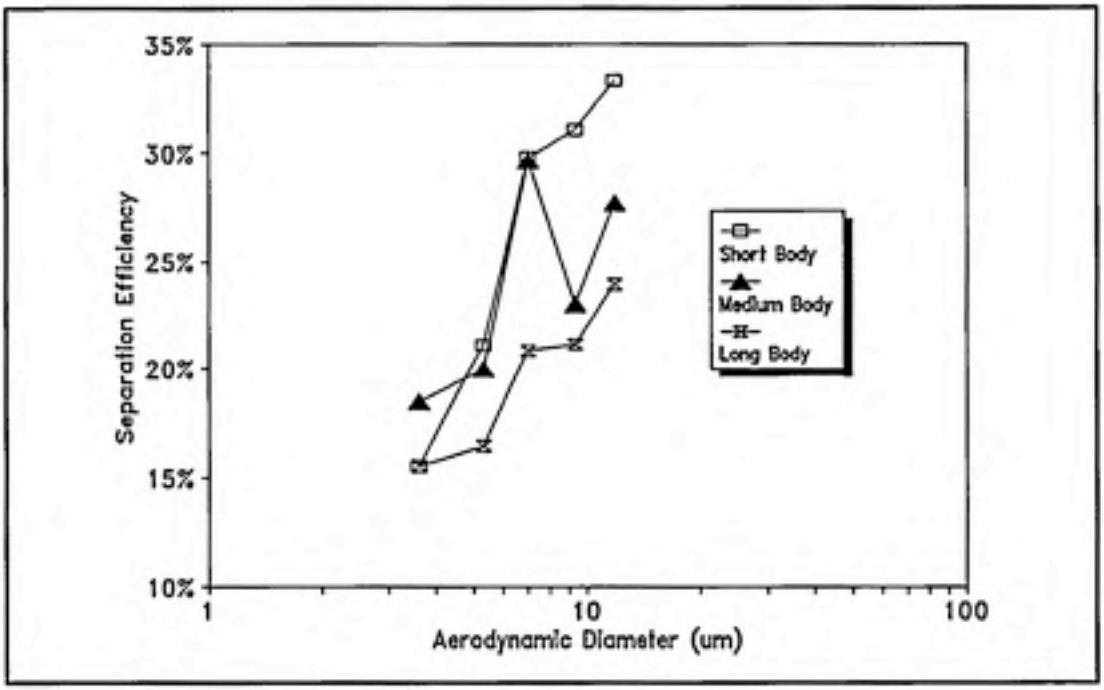

Figure 5.2: Separation Efficiency for the Thin Helix Design at Various Cyclone Body Tube Lengths

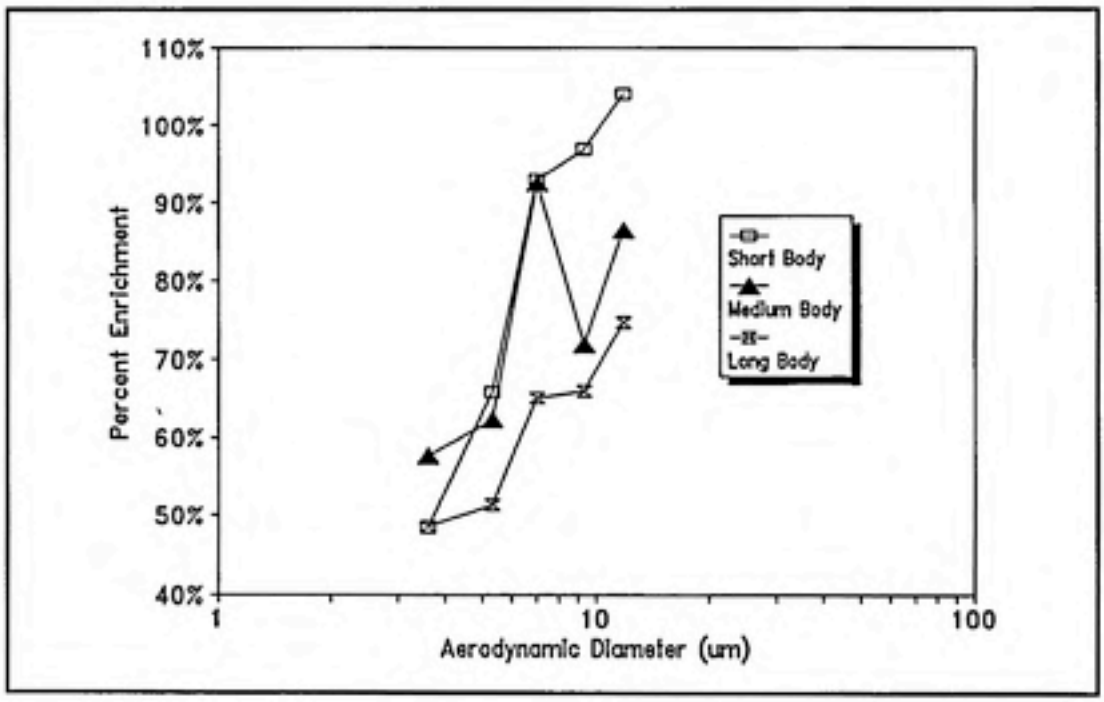

Figure 5.3: Percent Enrichment for the Thin Helix Design at Various Cyclone Body Tube Lengths

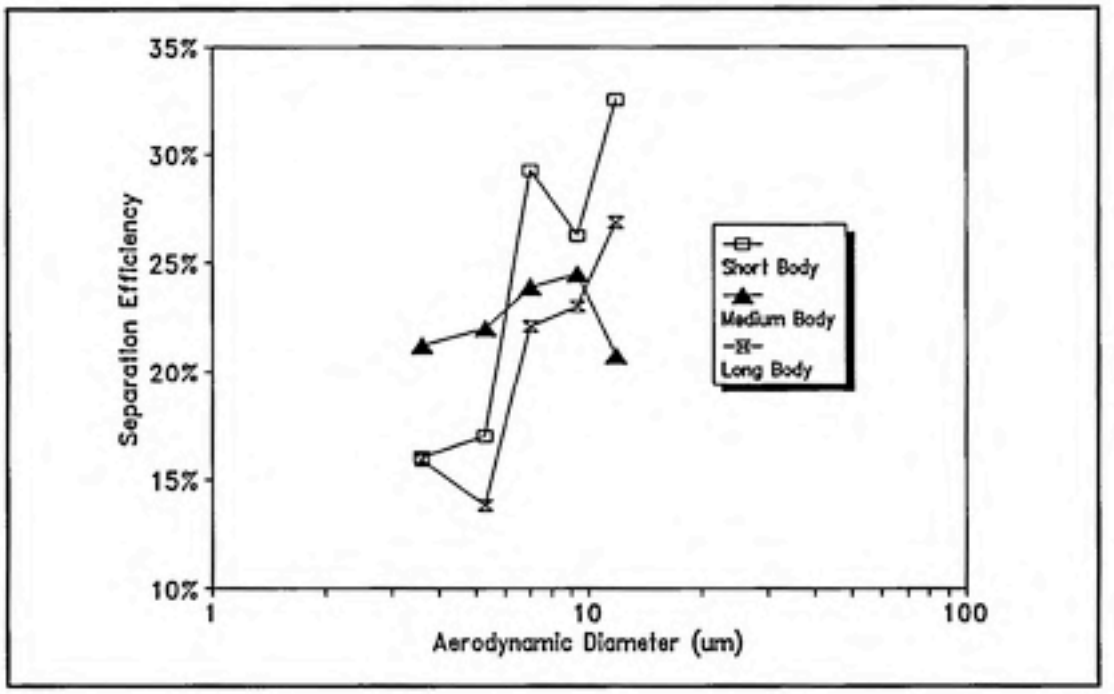

Figure 5.4: Separation Efficiency for the Wide Helix Design at Various Cyclone Body Tube Lengths

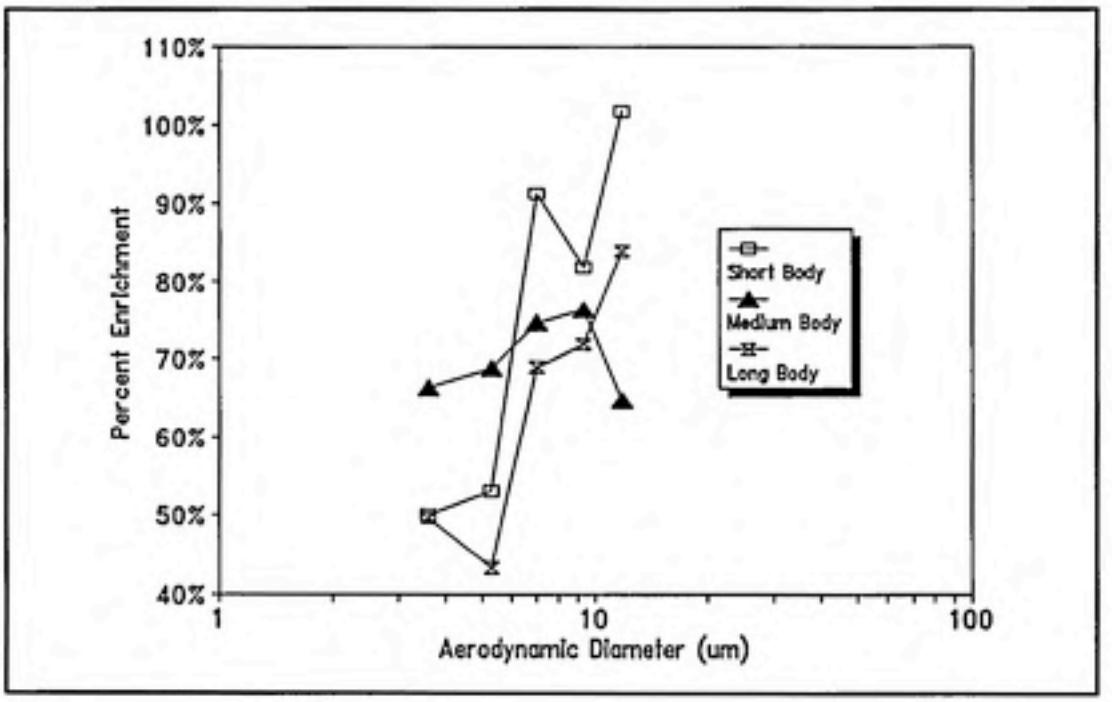

Figure 5.5: Percent Enrichment for the Wide Helix Design at Various Cyclone Body Tube Lengths

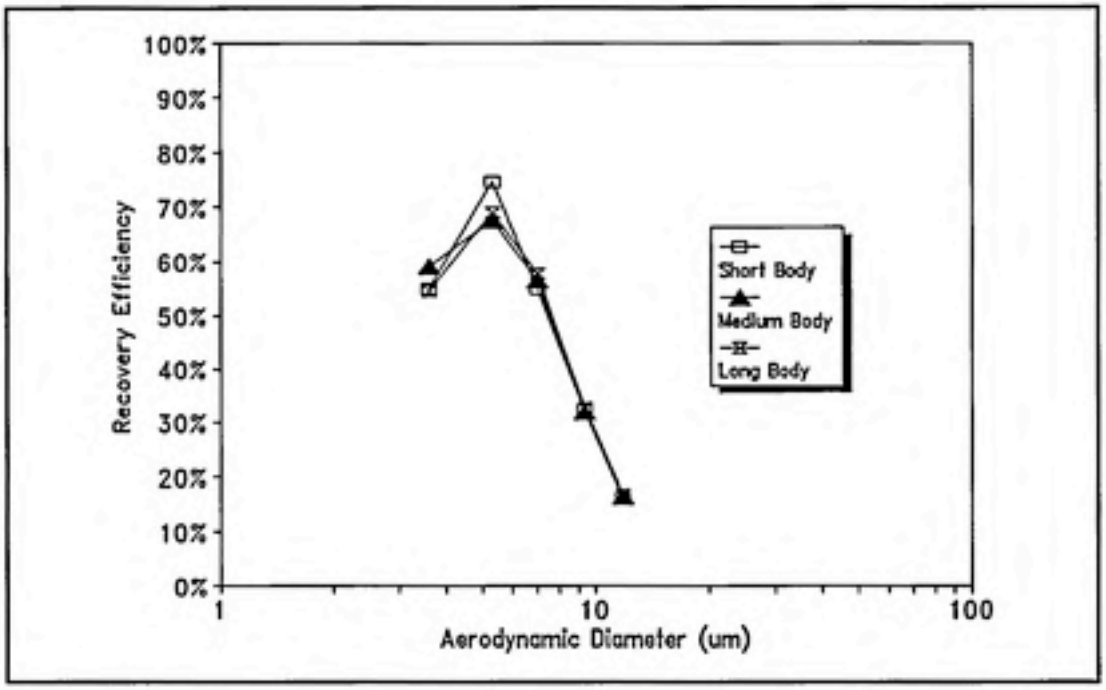

Figure 5.6: Recovery Efficiency for the Thin Helix Design at Various Cyclone Body Tube Lengths

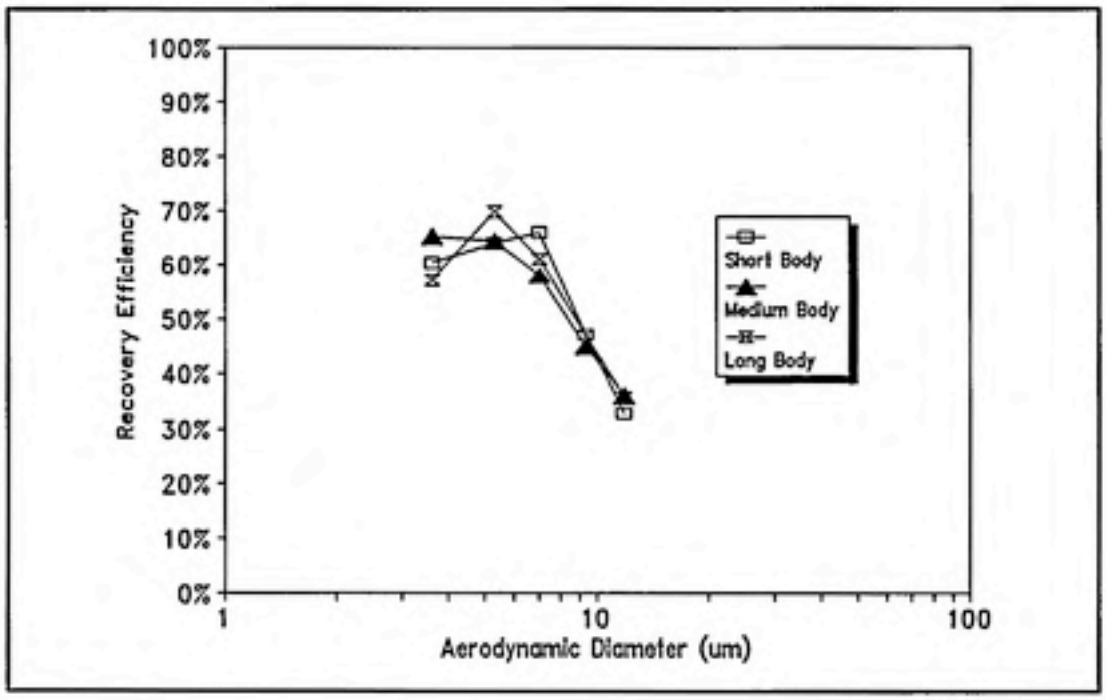

Figure 5.7: Recovery Efficiency for the Wide Helix Design at Various Cyclone Body Tube Lengths

and/or particle size) would imply at least two populations with different means.

A three-way ANOVA was used to determine variation of the particle concentration means of the various cyclone configurations using the response variable SEPEFF. First, the null hypothesis of no bias is tested by reference to the F-ratio for all effects in the model, i.e. helix design, cyclone tube length, the particle size effect, and the intercept. Lack of significance at the 0.05 level indicates no statistical difference of the population means. No further statistical testing is conducted in this case. A significant F-ratio indicates the presence of some bias. If this test indicates the presence of a bias, it could be a consistent bias of the same magnitude for all helix designs, cyclone tube lengths, and particle sizes or that the level of bias varies among the two helix designs, three cyclone tube lengths, and/or five particle sizes. A significant helix design, cyclone tube length, and/or particle size indicates the latter condition.

The results from the statistical analyses indicate that the overall bias was significant ($p<0.001$) and the variation of bias by cyclone tube length and particle size were significant ($p=0.004$ and $p<0.001$, respectively). However, the effect of helix design was not statistically significant at the 0.05 level ($p=0.512$). In addition, the interaction terms for the model (including helix design, cyclone tube length, and particle size) were not

significant at the 0.05 level ($p = 0.754$).

Based on these analyses and observation of the accompanying figures and table, the cyclone is capable of separating particles based on their aerodynamic diameter for the particle size ranges investigated. From Figure 5.2 and Figure 5.4, the most pronounced increasing trend is for the shortest cyclone body tube length for the thin or wide helix design, in either case the separation efficiency ranges from approximately 15% to 33%. In contrast, the long cyclone body tube shows a gradual increase in the separation efficiency, ranging from approximately 15% to 24%, for the thin helix design, and 27%, for the wide helix design. The medium cyclone body tube length shows the smallest variation in the separation efficiency for particle sizes ranging from 3.6 to 11.8 μm. Based on these results, it would appear that the short cyclone body tube length provides the optimum environment for separation of particles for the cyclone conditions studied. Helix design appears not to have an effect, either statistically or observationally.

Using a variation of Equation 5, it is possible to theoretically predict the separation efficiency of the cyclone at each particle size used in the cyclone configuration study. Correcting the velocity at the inlet for the angle (θ) of the helix, 5°, the separation efficiency (ϵ) can be expressed as:

$$\epsilon = \frac{L v_c d_p^2 \rho_p C_c \cos\theta}{9 D \mu B_c \tan\theta} \qquad (13)$$

where L is the cyclone body tube length, v_c is the cyclone inlet velocity, ρ_p is the density of the particle, C_c is the Cunningham slip correction factor, d_p is the aerodynamic diameter of the particle, μ is the viscosity of the air, and B_c is width of the helix entry cross-section.

Using the dimensional specifications of the experimental cyclone, the separation efficiency based on the theoretical equation is shown plotted in Figure 5.8. For the short cyclone body tube length and wide helix design, the separation efficiency as predicted by Equation 13 approaches that found in the experimental design for the same cyclone configuration. As the particle size decreases, the separation efficiency as predicted by theory under-estimates the particle concentration from the experiment. For the medium and long cyclone body tube lengths, the separation efficiencies at the larger particle sizes drastically over-estimate the particle concentrations observed in the experiment. Equation 13 assumes that the air streams in the cyclone retain the entry angle of the helix, hence the number of flow pattern rotations becomes a function of the cyclone body tube length and the entry angle. Realistically, once the incoming flow of air has exited the helical insert, the flow patterns may vary drastically from that assumed by simple theory. As the particle size decreases, the theoretical separation

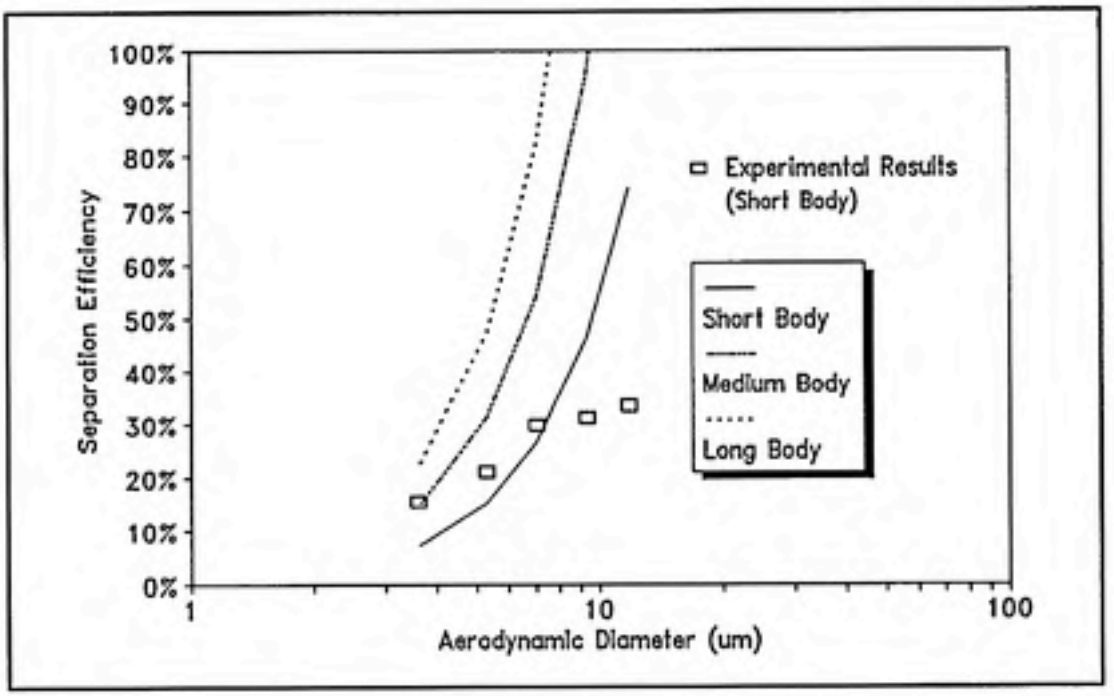

Figure 5.8: Theoretical Separation Efficiency for Cyclone Sampling Inlet

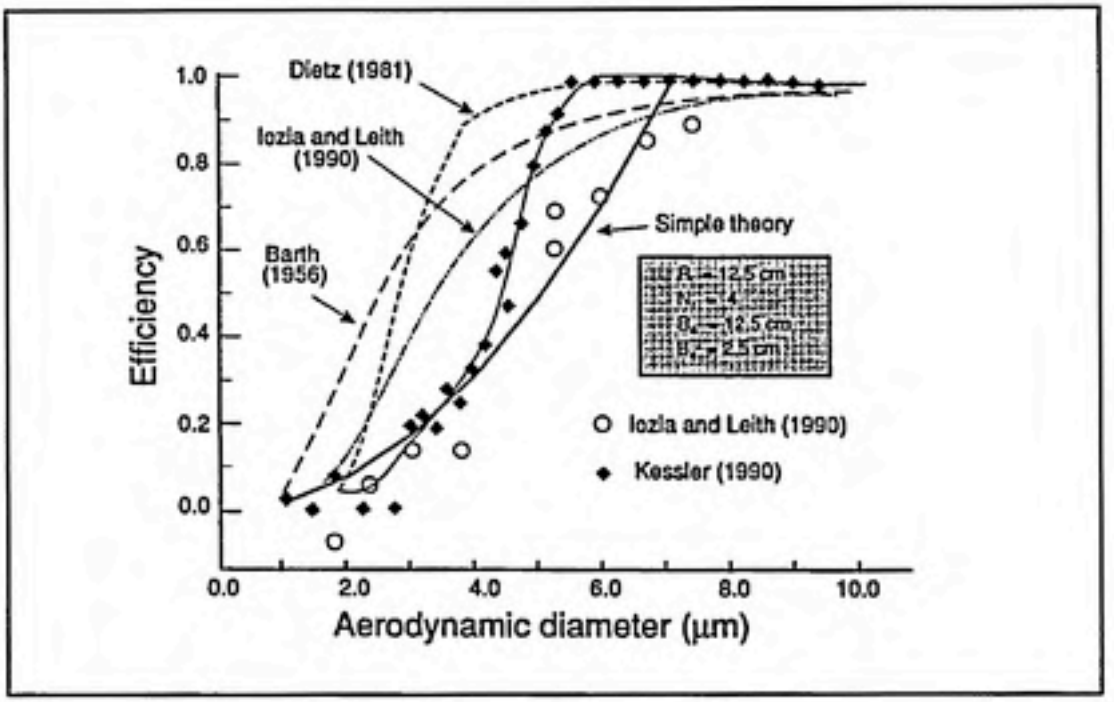

Figure 5.9: Comparison of Simple Theory with Detailed Theoretical Efficiency and Experimental Data

efficiencies begin to approach those experienced in the study. These observations support the original premise that a reduction of the sampler flow rate would shift the cut-off diameter to the right. Equation 13 cannot be expected to provide an accurate characterization of the cyclone separation efficiencies because it is based on simple theory. Theoretical separation efficiencies can predict a "ball-park" for the cyclone operation. Personal communication with Reist [1991] references a study conducted by Kessler [1990] which compares simple theory with detailed theoretical efficiency and experimental data for industrial cyclones, Figure 5.9. For Figure 5.9, the relationship between simple theory and experimental data is consistent with the results of this study.

5.2.2 Statistical Analyses of the Cyclone Recovery Efficiency

The statistical analyses used to assess the effect of the various cyclone configurations on the recovery efficiency of the system were the same as those used in the variable flow rate experiment. Analysis was conducted on the response variable RECEFF0 (corresponding the recovery efficiency of the system) using helix design, cyclone tube length, and particle size as predictors. Systematic differences in measurements (bias due to helix design, cyclone tube length, and/or particle size) would imply at least two populations with different means. A three-way ANOVA was used to determine (1) bias for all effects in the model, (2) a consistent bias among all effects, (3) bias that varies among the effects, and (4) a consistent bias for

the intercept. In a separate analysis, the variable BLCKCAT was added to the model to evaluate the statistical significance of similar experimental conditions being experienced on different days (separate experimental blocks).

The results from the statistical analyses indicate that the overall bias was significant ($p<0.001$) and the variation of bias by helix design and particle size were significant ($p<0.001$). However, the effect of cyclone tube length was not statistically significant at the 0.05 level ($p=0.992$). The interaction terms for the model (including helix design, cyclone tube length, and particle size) were marginally significant at the 0.05 level ($p=0.047$). The mean bias was negative, at the 0.05 significance level ($p<0.001$), indicating that the cyclone underestimates the filter cassette. When the effect for blocking was added to the model, the other significance factors remained consistent with the previous analyses. Blocking was not significant at the 0.05 level ($p=0.523$) indicating no statistical difference for similar experimental conditions on separate days.

Consistent with the flow rate experiment, as the diameter of particles challenging the cyclone is increased, the resultant recovery efficiency is decreased. This fact combined with the decrease in recovery efficiency for the thin helix inlet, as opposed to the wide helix inlet, indicate that even at the reduced flow rate, the entry lip to the helix is acting as an impaction

by fluorometric methods, is based on the total oleic acid present on the filter as a function of the mass of uranine (particle count is proportional to the inverted cube of the aerodynamic diameter). An over-estimate of the aerodynamic diameter, VOMAG diameter larger than APS diameter, would result in a lower particle count on the filter. At a particle size of 7 μm, the particle concentration (Figure 5.10) is fairly constant which is consistent with the close aerodynamic diameters detected by the APS between sampling blocks "a" and "b" (Figure 5.11).

The aerodynamic diameters predicted by the VOMAG were assumed to remain constant since the same oleic acid/uranine/alcohol solutions were used throughout the entire study. All solutions were kept in a dark environment, when not being used, to minimize the potential for fluorescence degradation from exposure to direct light. However, if the reduction in the chamber particle concentration was a result of the photo-decomposition of the uranine over time, the presentation of the results as ratios (i.e. separation efficiency and recovery efficiency) would normalize the data to reduce the bias introduced by this effect.

device (refer to Figures 5.4 and 5.5). The degree of this effect is reduced as particle size is decreased which is consistent with impactor theory as defined by the Stokes number (recall Equation 1).

5.2.3 Statistical Analyses of 47-mm Filter Cassette and APS Data

Statistical tests were conducted to determine the variability of the particle concentration in the aerosol chamber as "seen" by the 47-mm filter cassette and the APS. These tests were similar to those used in the variable flow rate experiment. Analyses were conducted on the response variable QCEFF0 (corresponding the ratio between the filter cassette and the APS minus 1) using particle size and sampling block as predictors. Systematic differences in measurements (bias due to particle size and/or sampling block) would imply at least two populations with different means. A two-way ANOVA was used to determine (1) bias for all effects in the model, (2) a consistent bias among all effects, (3) bias that varies among the effects, and (4) a consistent bias for the intercept. These same tests were also used on the data from the filter cassette and APS independently determine particle concentration variability of each sampling instrument apart from the other.

The results from the statistical analyses indicate that the overall bias was significant ($p<0.001$) and the variation of bias by particle size and sampling block were significant ($p<0.001$). The mean bias was negative, at the 0.05 significance level ($p<0.001$), indicating that the filter cassette

underestimates the APS for these experimental conditions. In addition, the interaction term for the model was significant at the 0.05 level ($p<0.001$). However, when the filter cassette and the APS were statistically analyzed independently, the effect of blocking, for the APS alone, was not significant ($p=0.336$).

The effect of particle size on the particle concentration, for the filter cassette and the APS, is consistent with the operating characteristics of the aerosol chamber. Larger diameter particles will be influenced to a greater degree by the effects of impaction onto the chamber baffles (due to the turbulent motion of the air) and elutriation as evidenced in Figure 5.10. For the filter cassette, the particle concentration between experimental sampling blocks is similar for aerodynamic diameters greater than 7 μm. For diameters less than 7 μm, there is a large variation between average block particle concentration. Observation of Figure 5.11, a plot of VOMAG predicted aerodynamic diameter versus the aerodynamic diameter detected by the APS, indicates smaller diameters at all particle size levels (with the exception of particle diameters at 7 μm) for sampling block "a" as opposed to block "b". For particle diameters smaller than 7 μm, this decrease in the second block is more pronounced. This drop in the particle size for the second sampling block, observed by the APS, may account for a large part of the decrease in the filter cassette particle concentration. The calculation of the particle concentration, for the filter cassette and subsequent analysis

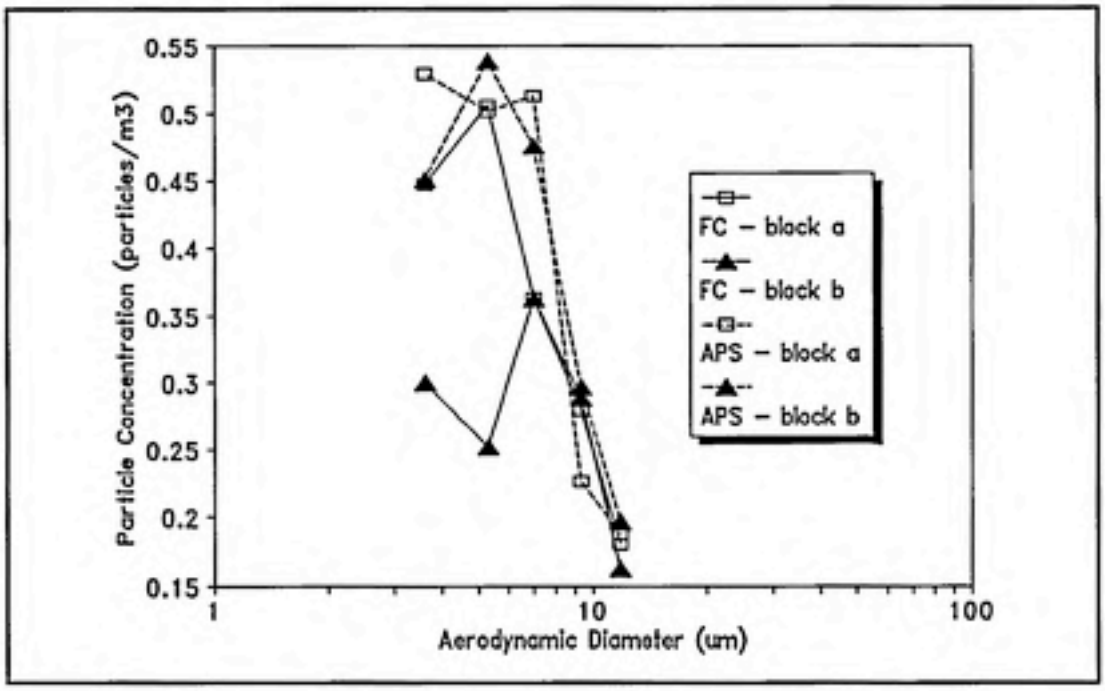

Figure 5.10: Particle Concentration versus Aerodynamic Diameter for 47-mm Filter Cassette and APS

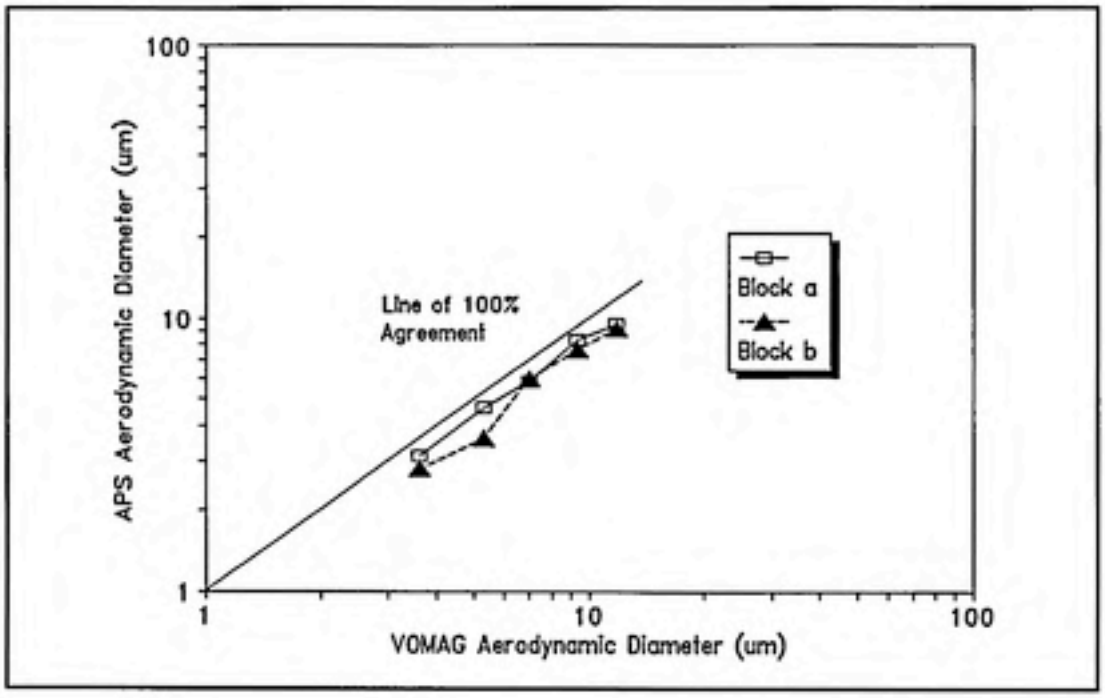

Figure 5.11: VOMAG Predicted Aerodynamic Diameter Versus APS Detected Particle Size

VI CONCLUSIONS

Under the imposed conditions of this investigation, the cyclone sampling inlet appears capable of separating particles as a function of their aerodynamic diameter. However, the realization of the 50% effective cut-off diameter at 8 μm was not observed primarily due to the reduction of the sampler flow rate from the original design specifications. The reduction of the flow rate to 7 lpm improved the recovery efficiency of the cyclone system but also had the added effect of shifting the d_{50} to a particle size greater than 8 μm. Assuming a linear relationship between the aerodynamic particle diameter and the separation efficiency, regressions on the results of both helix designs and a short body tube length, indicate extrapolated d_{50} values of 18.5 and 20.2 μm for the thin and wide helical inserts, respectively. The reduction of the sampler flow rate also increased the particle impactor cut-size (100% particle collection) at the exit slit from the designed value of 1 μm to 2.4 μm. The greatest improvements in the recovery efficiencies occurred for aerodynamic particle diameters less than 7 μm. Increasing particle diameters above 7 μm showed a propensic reduction in the recovery efficiencies which supports the conclusion of continued particle impaction at the helix entry.

The short body tube length, for both helix designs, showed the most

consistent separation of particles for increasing aerodynamic particle diameters ranging from 15% to 33%. For the medium and long body tube lengths, both helix designs, the increase in separation efficiency for increases in aerodynamic particle diameter were not as pronounced. Theoretically, longer body tube lengths should exhibit greater separation efficiencies based on the increased number of turns made by the moving air mass in the cyclone interior. The inconsistency of the data with this theoretical concept indicates that the moving air mass does not retain the rotational component past the helical insert. The width of the helical insert cross-sectional area did not have statistically significant effect on the particle separation efficiency.

Redesign of helical insert is needed to shift the d_{50} back to the designed particle diameter cut size of 8 μm. However, the original shift in the d_{50}, observed in the various cyclone configurations experiment, was caused primarily by the reduction of the sampling inlet flow rate. The flow rate was reduced to increase the sampling efficiency of the system. Recall, from the flow rate experiment, that at a flow rate of 28 lpm, a deposit of uranine was observed below the helix entry lip indicating inertial particle impaction caused by the air stream changes into the entry. The redesign of the helical insert must therefore incorporate the optimization of the sampling efficiency so that the sampling inlet can be used at the increased flow rate of 28 lpm required by the Mattson-Garvin slit-to-agar bioaerosol sampler. Increasing

the helix channel depth and tapering the entry into the helix should provide entry conditions that minimize the effect of particle impaction. To provide more rotations of the air mass, hence, greater particle separation, the helical insert can be machined with a greater number of turns. If a sampler flow rate of 28 lpm proves to be limiting to the sampling efficiency of the system for future entry designs, then a lower flow rate may be used as long as the exit slit is redesigned to accommodate the volumetric air flow reduction.

REFERENCES

Andersen Samplers, Inc., Operating Manual Andersen Samplers Inc. Viable (Microbial) Particle Sizing Samplers, Atlanta, Georgia, TR No. 76-900042, 1976.

Akiyama, T. and Marui, T., "Dust Collection Efficiency of a Straight-through Cyclone: Effects of Duct Length, Guide Vanes and Nozzle Angle for Secondary Rotational Air Flow", Powder Technology,58:181-185, 1989.

Ananth, G. and Wilson, J., "Theoretical Analysis of the Performance of the TSI Aerodynamic Particle Sizer: The Effect of Density on Response", Aerosol Science and Technology, 9:189-199, 1988.

ASHRAE Handbook: 1983 Equipment Volume, "Chapter 10: Air Cleaners", Third Printing, Atlanta, Georgia, 1985.

Baron, P., "Calibration and Use of the Aerodynamic Particle Sizer (APS 3000)", Aerosol Science and Technology, 5:55-67, 1986.

Berglund, R., "Basic Aerosol Standards and Optical Measurements of Aerosol Particles", Masters Thesis, University of Minnesota, June 1972.

Berglund, R., and Liu, B., "Generation of Monodisperse Aerosol Standard," Environmental Science and Technology, 7(2):147-153, 1973.

Burnard, G., "The Development of a Precleaner Which is Compatible with the MRDE High Capacity Dust Collector", The Mining Engineer, pages 461-464, April 1988.

Caplan, K., "Source Control by Centrifugal Force and Gravity", Air Pollution: Engineering Control of Air Pollution, Stern, A., editor, Third Edition, Volume IV, 97-148.

Chen, B., Cheng, Y., and Yeh, H., "Performance of a TSI Aerodynamic Particle Sizer", Aerosol Science and Technology, 4:89-97, 1985.

Fairfield, C., Tillery, M., Smith, J., and Valdez, F., "Collection Efficiency of Field Sampling Cassettes", National Institute for Occupational Safety and Health, Report No. LA-8640-MS/UC-41, December 1980.

Gressel, M., Heitbrink, W., McGlothlin, J., and Fischbach, T., "Advantages of Real-Time Data Acquisition for Exposure Assessment", Applied Industrial Hygiene, 3(11):316-320, 1988.

Griffiths, W., Iles, P., and Vaughn, N., "The Behavior of Liquid Droplet Aerosols in an APS 3000", Journal of Aerosol Science, 17(6):921-930, 1986.

Guilbault, G., Practical Fluorescence: Theory, Methods, and Techniques, Marcel Dekker, Inc., New York, New York, 1973.

Hercules, D., Fluorescence and Phosphorescence Analysis, Interscience Publishers, New York, 1966.

Hinds, W. and Kraske, G., "A Bench-scale Aerosol Test Chamber", Applied Industrial Hygiene, 2(1):13-17, 1987.

Hinds, W., Aerosol Technology: Properties, Behavior, and Measurement of Airborne Particles, John Wiley and Sons, New York, New York, 1982.

Jensen, P., Davis, G., and Todd, W., "Evaluation of Sampling Alternatives for Bioaerosols Phase II: Viable Microorganism Sampling Efficiency", National Institute for Occupational Safety and Health, Cincinnati, Ohio, 1991.

Kotimaa, M., Husman, K., Terho, E., and Mustonen, M., "Airborne Molds and Actinomycetes in the Work Environment of Farmer's Lung Patients in Finland", Scandinavian Journal of Work and Environmental Health, 10:115-119, 1984.

Marple, V. and Rubow, K., "An Aerosol Chamber for Instrument Evaluation and Calibration", American Industrial Hygiene Association Journal, 44(5)361-367, 1983.

Martinez, K., Todd, W., and Fischbach, T., "Evaluation of Alternative Samplers for Bioaerosols Phase I: Physical Sampling Efficiency", National Institute for Occupational Safety and Health, Cincinnati, Ohio, 1991.

Martinez, K., Sheehy, J., Jones, J., and Cusick, L., "Microbial Containment in Conventional Enzyme Fermentation Processes", Applied Industrial Hygiene, 3(6):177-181, 1988.

O'Brien, D., Fischbach, T., Cooper, T., Todd, W., Gressel, M., and Martinez, K., "Acquisition and Spreadsheet Analysis of Real Time Dust Exposure Data: A Case Study", Applied Industrial Hygiene, 4(9):238-243, 1989.

Ogawa, A., "Estimation of the Collection Efficiencies of the Three Types of the Cyclone Dust Collectors from the Standpoint of the Flow Patterns in the Cylindrical Cyclone Dust Collectors", Bulletin of JSME, 27(233):64-69, January 1984.

Perkin-Elmer Model 650-10S Fluorescence Spectrophotometer Operators Manual, The Perkin-Elmer Corporation, Norwalk, Connecticut, June 1978.

Reist, P., Introduction to Aerosol Science, Macmillan Publishing Company, New York, New York, 1984.

Ström, G. and Blomquist, G., "Airborne Spores from Mouldy Citrus Fruit - A Potential Occupational Health Hazard", Annals of Occupational Hygiene, 30(4):455-460, 1986.

Tenney, E., "Upgrading Performance of Mechanical Dust Collectors", Plant Engineering, pages 99-102, February 21, 1980.

Topping, M., Scarisbrick, D., Luczynska, C., Clarke, E., and Seaton, A., "Clinical and Immunological Reaction to *Aspergillus niger* Among Workers at a Biotechnology Plant", British Journal of Industrial Medicine, 42:312-318, 1985.

Tseng, L., "Optimization of the Uranine Wash-off Method for Measuring Aerosol Concentrations", Masters Technical Report, University of North Carolina, Chapel Hill, North Carolina, 1991.

Underfriend, S., Fluorescence Assay in Biology and Medicine, Volume I & II, Academic Press, New York, 1962.

Vaughn, N., "Construction and Testing of an Axial Flow Cyclone Preseparator", Journal of Aerosol Science, 19(3):295-305, 1988.

Vincken, W. and Roels, P., "Hypersensitivity Pneumonitis Due to *Aspergillus fumigatus* in Compost", Thorax, 39:74-75, 1984.

Walters, P., Moore, M. and Webb, A., "A Separator for Obtaining Samples of Cloud Water in Aircraft", Atmospheric Environment, 17(6):1083-1091, 1983.

Willeke, K., "Performance of the Slotted Impactor", American Industrial Hygiene Association Journal, pages 683-691, September 1975.

APPENDIX

The appendix presents the raw data from the variable flow rate experiment and the various cyclone configurations experiment. The title labels are fairly self-explanatory. Helix Design refers to the width of the helical insert inlet with "1" corresponding to the thin inlet and "2" corresponding to the wide inlet. Cyclone Length refers to the length of the cyclone body tube with "1" corresponding to the short tube, "2" corresponding to the medium tube, and "3" corresponding to the long tube. PM Gain and Sensitivity Range refer to the photomultiplier tube gain and sensitivity setting, respectively, on the Perk-Elmer fluorescence spectrophotometer. Corrected Concentration refers to blank corrected uranine concentration (per milliliter of 0.01 N NaOH) on the filters.

VARIABLE FLOW RATE EXPERIMENT

FILTER NO.	HELIX DESIGN	CYCLONE LENGTH	PARTICLE SIZE (um)	FLOW RATE (lpm)	FLUORESCENCE READING CUVET 1	CUVET 2	AVERAGE	PM GAIN	SENSITIVITY RANGE	TRUE READING	CONCENTRATION URANINE (ug/ml)	CORRECTED CONC (ug/ml)	APS CONC (part/cm3)
BLANK12a1			0	0	68	78	73	Normal	30	2.43	1.83E-05	3.18E-06	0
FCYC12-1a	2	2	14.14	28	85	95	90	Normal	10	9.00	6.01E-05	4.49E-05	0.091
FCYC12-2a	2	2	14.14	7	54.2	54.5	54.35	Normal	0.1	543.50	3.46E-03	3.44E-03	0.0968
FCYC12-3a	2	2	14.14	14	85	86	85.5	Normal	10	8.55	5.72E-05	4.21E-05	0.0989
FCYC12-4a	2	2	14.14	14	73	74	73.5	Normal	10	7.35	4.96E-05	3.45E-05	0.0918
FCYC12-5a	2	2	14.08	28	32.5	33.3	32.9	Normal	3	10.97	7.26E-05	5.75E-05	0.095
FCYC12-6a	2	2	14.08	7	76	75.7	75.85	Normal	0.1	758.50	4.83E-03	4.81E-03	0.0983
FCYC12-7a	2	2	14.08	14	43.4	44.3	43.85	Normal	3	14.62	9.58E-05	8.07E-05	0.0979
FCYC12-8a	2	2	14.08	28	65	61	63	Normal	10	6.30	4.29E-05	2.78E-05	0.0993
FCYC12-9a	2	2	14.08	7	102.5	102.5	102.5	Normal	0.1	1025.00	6.52E-03	6.51E-03	0.102
BLANK12a2			0	0	44	50	47	Normal	30	1.57	1.28E-05	-2.33E-06	0
FFC12-1a	2	2	14.14	14	102.5	102.3	102.4	Low	0.3	341.33	3.22E-02	3.22E-02	0.091
FFC12-2a	2	2	14.14	14	113.2	112	112.6	Low	0.3	375.33	3.54E-02	3.54E-02	0.0968
FFC12-3a	2	2	14.14	14	114.1	113.9	114	Low	0.3	380.00	3.58E-02	3.58E-02	0.0989
FFC12-4a	2	2	14.14	14	105.1	105.4	105.25	Low	0.3	350.83	3.31E-02	3.31E-02	0.0918
FFC12-5a	2	2	14.08	14	53.7	53.8	53.75	Low	0.1	537.50	5.07E-02	5.06E-02	0.095
FFC12-6a	2	2	14.08	14	57.2	56.9	57.05	Low	0.1	570.50	5.38E-02	5.38E-02	0.0983
FFC12-7a	2	2	14.08	14	60.2	60.2	60.2	Low	0.1	602.00	5.67E-02	5.67E-02	0.0979
FFC12-8a	2	2	14.08	14	59.1	59	59.05	Low	0.1	590.50	5.57E-02	5.56E-02	0.0993
FFC12-9a	2	2	14.08	14	64.7	64.6	64.65	Low	0.1	646.50	6.09E-02	6.09E-02	0.102
BLANK8a1			0	0	45	57	51	Normal	30	1.70	1.36E-05	-1.48E-06	0
FCYC8-1a	2	2	9.34	7	110.9	111	110.95	Low	1	110.95	1.05E-02	1.05E-02	0.267
FCYC8-2a	2	2	9.34	14	44	44.5	44.25	Normal	0.1	442.50	2.82E-03	2.80E-03	0.263
FCYC8-3a	2	2	9.34	28	65	63	64	Normal	10	6.40	4.35E-05	2.84E-05	0.264
FCYC8-4a	2	2	9.34	28	50	47	48.5	Normal	10	4.85	3.37E-05	1.86E-05	0.26
FCYC8-5a	2	2	9.34	14	47.8	48.1	47.95	Normal	0.1	479.50	3.05E-03	3.04E-03	0.257
FCYC8-6a	2	2	9.36	7	110	110.8	110.4	Low	1	110.40	1.04E-02	1.04E-02	0.257
FCYC8-7a	2	2	9.36	14	51.1	51.5	51.3	Normal	0.1	513.00	3.27E-03	3.25E-03	0.258
FCYC8-8a	2	2	9.36	7	113.1	112.6	112.85	Low	1	112.85	1.07E-02	1.07E-02	0.257
FCYC8-9a	2	2	9.36	28	56.3	57.1	56.7	Normal	3	18.90	1.23E-04	1.08E-04	0.257
BLANK8a2			0	0	75	64	69.5	Normal	30	2.32	1.75E-05	2.44E-06	0
FFC8-1a	2	2	9.34	14	114.4	114.8	114.6	Low	0.3	382.00	3.60E-02	3.60E-02	0.267
FFC8-2a	2	2	9.34	14	101.5	101.8	101.65	Low	0.3	338.83	3.20E-02	3.19E-02	0.263
FFC8-3a	2	2	9.34	14	120.3	120.7	120.5	Low	0.3	401.67	3.79E-02	3.79E-02	0.264
FFC8-4a	2	2	9.34	14	120.3	122.4	121.35	Low	0.3	404.50	3.81E-02	3.81E-02	0.26
FFC8-5a	2	2	9.34	14	122.1	121.9	122	Low	0.3	406.67	3.83E-02	3.83E-02	0.257
FFC8-6a	2	2	9.36	14	119.5	117.8	118.65	Low	0.3	395.50	3.73E-02	3.73E-02	0.257
FFC8-7a	2	2	9.36	14	119	118.8	118.9	Low	0.3	396.33	3.74E-02	3.74E-02	0.258

VARIABLE FLOW RATE EXPERIMENT

FILTER NO.	HELIX DESIGN	CYCLONE LENGTH	PARTICLE SIZE (um)	FLOW RATE (lpm)	FLUORESCENCE READING CUVET 1	CUVET 2	AVERAGE	PM GAIN	SENSITIVITY RANGE	TRUE READING	CONCENTRATION URANINE (ug/ml)	CORRECTED CONC (ug/ml)	APS CONC (part/cm3)
FFC8-8a	2	2	9.36	14	120.6	120.3	120.45	Low	0.3	401.50	3.79E-02	3.78E-02	0.257
FFC8-9a	2	2	9.36	14	122.2	122.2	122.2	Low	0.3	407.33	3.84E-02	3.84E-02	0.257
BLANK3a1			0	0	46	46	46	Normal	30	1.53	1.26E-05	-2.54E-06	0
FCYC3-1a	2	2	3.54	28	43.8	44.1	43.95	Normal	0.1	439.50	2.80E-03	2.78E-03	0.453
FCYC3-2a	2	2	3.54	14	41.2	41.4	41.3	Normal	0.1	413.00	2.63E-03	2.61E-03	0.464
FCYC3-3a	2	2	3.54	7	68.5	68.7	68.6	Normal	0.3	228.67	1.46E-03	1.44E-03	0.469
FCYC3-4a	2	2	3.54	14	42.1	42.2	42.15	Normal	0.1	421.50	2.68E-03	2.67E-03	0.478
FCYC3-5a	2	2	3.54	7	67.8	68.2	68	Normal	0.3	226.67	1.44E-03	1.43E-03	0.43
FCYC3-6a	2	2	3.54	28	42.7	42.8	42.75	Normal	0.1	427.50	2.72E-03	2.71E-03	0.446
FCYC3-7a	2	2	3.54	28	46	46.1	46.05	Normal	0.1	460.50	2.93E-03	2.92E-03	0.451
FCYC3-8a	2	2	3.54	7	79.6	79.9	79.75	Normal	0.3	265.83	1.69E-03	1.68E-03	0.465
FCYC3-9a	2	2	3.54	14	47.6	47.7	47.65	Normal	0.1	476.50	3.03E-03	3.02E-03	0.468
FCYC3-10a	2	2	3.54	28	48.8	48.9	48.85	Normal	0.1	488.50	3.11E-03	3.09E-03	0.457
BLANK3a2			0	0	54	62	58	Normal	30	1.93	1.51E-05	2.82E-22	0
FFC3-1a	2	2	3.54	14	44	44.1	44.05	Normal	0.1	440.50	2.80E-03	2.79E-03	0.453
FFC3-2a	2	2	3.54	14	62	61.7	61.85	Normal	0.1	618.50	3.94E-03	3.92E-03	0.464
FFC3-3a	2	2	3.54	14	60.8	60.8	60.8	Normal	0.1	608.00	3.87E-03	3.86E-03	0.469
FFC3-4a	2	2	3.54	14	60.7	60.8	60.75	Normal	0.1	607.50	3.87E-03	3.85E-03	0.478
FFC3-5a	2	2	3.54	14	59.7	60	59.85	Normal	0.1	598.50	3.81E-03	3.79E-03	0.43
FFC3-6a	2	2	3.54	14	58.2	58.3	58.25	Normal	0.1	582.50	3.71E-03	3.69E-03	0.446
FFC3-7a	2	2	3.54	14	60	59.8	59.9	Normal	0.1	599.00	3.81E-03	3.80E-03	0.451
FFC3-8a	2	2	3.54	14	54	53.9	53.95	Normal	0.1	539.50	3.43E-03	3.42E-03	0.465
FFC3-9a	2	2	3.54	14	61.2	61.7	61.45	Normal	0.1	614.50	3.91E-03	3.90E-03	0.468
FFC3-10a	2	2	3.54	14	62.8	63	62.9	Normal	0.1	629.00	4.00E-03	3.99E-03	0.457
FFC3-11a	2	2	3.54	14	61.5	61.3	61.4	Normal	0.1	614.00	3.91E-03	3.89E-03	0.442
BLANK8b1			0	0	73	49	61	Normal	30	2.03	1.57E-05	6.36E-07	0
FCYC8-1b	2	2	9.41	14	55.9	56	55.95	Normal	0.1	559.50	3.56E-03	3.55E-03	0.228
FCYC8-2b	2	2	9.41	28	62	67	64.5	Normal	10	6.45	4.38E-05	2.87E-05	0.232
FCYC8-3b	2	2	9.41	7	37.2	37.3	37.25	Low	0.3	124.17	1.17E-02	1.17E-02	0.244
FCYC8-4b	2	2	9.41	7	32	31.9	31.95	Low	0.3	106.50	1.01E-02	1.01E-02	0.24
FCYC8-5b	2	2	9.33	28	81.5	84.5	83	Normal	3	27.67	1.79E-04	1.64E-04	0.234
FCYC8-6b	2	2	9.33	14	45	44.7	44.85	Normal	0.1	448.50	2.86E-03	2.84E-03	0.237
FCYC8-7b	2	2	9.33	14	47.7	47.7	47.7	Normal	0.1	477.00	3.04E-03	3.02E-03	0.229
FCYC8-8b	2	2	9.33	14	41.6	41.6	41.6	Normal	0.1	416.00	2.65E-03	2.63E-03	0.227
FCYC8-9b	2	2	9.33	7	32.6	32.6	32.6	low	0.3	108.67	1.03E-02	1.03E-02	0.226
FCYC8-10b	2	2	9.33	28	103	115	109	Normal	30	3.63	2.59E-05	1.08E-05	0.24
BLANK8b2			0	0	56	43	49.5	Normal	30	1.65	1.33E-05	-1.80E-06	0
FFC8-1b	2	2	9.41	14	116.2	115.7	115.95	Low	0.3	386.50	3.64E-02	3.64E-02	0.228

VARIABLE FLOW RATE EXPERIMENT

FILTER NO.	HELIX DESIGN	CYCLONE LENGTH	PARTICLE SIZE (um)	FLOW RATE (lpm)	FLUORESCENCE READING CUVET 1	CUVET 2	AVERAGE	PM GAIN	SENSITIVITY RANGE	TRUE READING	CONCENTRATION URANINE (ug/ml)	CORRECTED CONC (ug/ml)	APS CONC (part/cm3)
FFC8-2b	2	2	9.41	14	116.1	116.3	116.2	Low	0.3	387.33	3.65E-02	3.65E-02	0.232
FFC8-3b	2	2	9.41	14	115.6	115.9	115.75	Low	0.3	385.83	3.64E-02	3.64E-02	0.244
FFC8-4b	2	2	9.41	14	115.8	117.4	116.6	Low	0.3	388.67	3.66E-02	3.66E-02	0.24
FFC8-5b	2	2	9.33	14	116.4	116.2	116.3	Low	0.3	387.67	3.66E-02	3.65E-02	0.234
FFC8-6b	2	2	9.33	14	113.8	114.6	114.2	Low	0.3	380.67	3.59E-02	3.59E-02	0.237
FFC8-7b	2	2	9.33	14	114.5	115.7	115.1	Low	0.3	383.67	3.62E-02	3.62E-02	0.229
FFC8-8b	2	2	9.33	14	117.3	117	117.15	Low	0.3	390.50	3.68E-02	3.68E-02	0.227
FFC8-9b	2	2	9.33	14	116.4	116.2	116.3	Low	0.3	387.67	3.66E-02	3.65E-02	0.226
FFC8-10b	2	2	9.33	14	115	114.7	114.85	Low	0.3	382.83	3.61E-02	3.61E-02	0.24
BLANK3b1			0	0	43	80	61.5	Normal	30	2.05	1.58E-05	7.42E-07	0
FCYC3-1b	2	2	3.56	14	42.9	42.9	42.9	Normal	0.1	429.00	2.73E-03	2.72E-03	0.46
FCYC3-2b	2	2	3.56	28	48.2	48.4	48.3	Normal	0.1	483.00	3.08E-03	3.06E-03	0.451
FCYC3-3b	2	2	3.56	7	73.8	74.6	74.2	Normal	0.3	247.33	1.58E-03	1.56E-03	0.479
FCYC3-4b	2	2	3.56	14	44	44.3	44.15	Normal	0.1	441.50	2.81E-03	2.80E-03	0.481
FCYC3-5b	2	2	3.56	7	69.9	69.8	69.85	Normal	0.3	232.83	1.48E-03	1.47E-03	0.485
FCYC3-6b	2	2	3.56	28	49	49.1	49.05	Normal	0.1	490.50	3.12E-03	3.11E-03	0.492
FCYC3-7b	2	2	3.56	14	44.2	44.2	44.2	Normal	0.1	442.00	2.81E-03	2.80E-03	0.499
FCYC3-8b	2	2	3.56	7	71.4	71.8	71.6	Normal	0.3	238.67	1.52E-03	1.51E-03	0.491
FCYC3-9b	2	2	3.56	28	46.7	47	46.85	Normal	0.1	468.50	2.98E-03	2.97E-03	0.492
FCYC3-10b	2	2	3.56	14	45.3	45.5	45.4	Normal	0.1	454.00	2.89E-03	2.88E-03	0.468
BLANK3b2			0	0	46	70	58	Normal	30	1.93	1.51E-05	2.82E-22	0
FFC3-1b	2	2	3.56	14	60.3	60.6	60.45	Normal	0.1	604.50	3.85E-03	3.83E-03	0.46
FFC3-2b	2	2	3.56	14	58.3	58.6	58.45	Normal	0.1	584.50	3.72E-03	3.71E-03	0.451
FFC3-3b	2	2	3.56	14	58	58	58	Normal	0.1	580.00	3.69E-03	3.68E-03	0.479
FFC3-4b	2	2	3.56	14	61	60.8	60.9	Normal	0.1	609.00	3.88E-03	3.86E-03	0.481
FFC3-5b	2	2	3.56	14	63.7	64.3	64	Normal	0.1	640.00	4.07E-03	4.06E-03	0.485
FFC3-6b	2	2	3.56	14	62.6	62.6	62.6	Normal	0.1	626.00	3.98E-03	3.97E-03	0.492
FFC3-7b	2	2	3.56	14	61.2	61.5	61.35	Normal	0.1	613.50	3.91E-03	3.89E-03	0.499
FFC3-8b	2	2	3.56	14	62.3	62.7	62.5	Normal	0.1	625.00	3.98E-03	3.96E-03	0.491
FFC3-9b	2	2	3.56	14	64.9	65	64.95	Normal	0.1	649.50	4.13E-03	4.12E-03	0.492
FFC3-10b	2	2	3.56	14	60.6	60.6	60.6	Normal	0.1	606.00	3.86E-03	3.84E-03	0.468
BLANK12a1			0	0	41	41	41	Normal	30	1.37	1.15E-05	-3.60E-06	0
FCYC12-1b	2	2	14.05	14	63	58	60.5	Normal	10	6.05	4.13E-05	2.62E-05	0.102
FCYC12-2b	2	2	14.05	7	61.9	61.8	61.85	Normal	0.1	618.50	3.94E-03	3.92E-03	0.103
FCYC12-3b	2	2	14.05	28	68	70	69	Normal	10	6.90	4.67E-05	3.16E-05	0.108
FCYC12-4b	2	2	14.05	14	48	50	49	Normal	10	4.90	3.40E-05	1.89E-05	0.111
FCYC12-5b	2	2	14.05	7	53.3	53.7	53.5	Normal	0.1	535.00	3.41E-03	3.39E-03	0.11
FCYC12-6b	2	2	14.15	28	70	76	73	Normal	10	7.30	4.92E-05	3.41E-05	0.107

VARIABLE FLOW RATE EXPERIMENT

FILTER NO.	HELIX DESIGN	CYCLONE LENGTH	PARTICLE SIZE (um)	FLOW RATE (lpm)	FLUORESCENCE READING CUVET 1	CUVET 2	AVERAGE	PM GAIN	SENSITIVITY RANGE	TRUE READING	CONCENTRATION URANINE (ug/ml)	CORRECTED CONC (ug/ml)	APS CONC (part/cm3)
FCYC12-7b	2	2	14.15	28	28	31	29.5	Normal	10	2.95	2.16E-05	6.47E-06	0.115
FCYC12-8b	2	2	14.15	7	38.8	38.9	38.85	Normal	0.1	388.50	2.47E-03	2.46E-03	0.12
FCYC12-9b	2	2	14.15	14	58	62	60	Normal	10	6.00	4.10E-05	2.59E-05	0.117
BLANK12b2			0	0	76	85	80.5	Normal	30	2.68	1.99E-05	4.77E-06	0
FFC12-1b	2	2	14.05	14	49	49.4	49.2	Low	0.1	492.00	4.64E-02	4.64E-02	0.102
FFC12-2b	2	2	14.05	14	45.3	45.3	45.3	Low	0.1	453.00	4.27E-02	4.27E-02	0.103
FFC12-3b	2	2	14.05	14	48	47.8	47.9	Low	0.1	479.00	4.52E-02	4.51E-02	0.108
FFC12-4b	2	2	14.05	14	49	48.7	48.85	Low	0.1	488.50	4.60E-02	4.60E-02	0.111
FFC12-5b	2	2	14.05	14	49	49.2	49.1	Low	0.1	491.00	4.63E-02	4.63E-02	0.11
FFC12-6b	2	2	14.15	14	53.2	53	53.1	Low	0.1	531.00	5.00E-02	5.00E-02	0.107
FFC12-7b	2	2	14.15	14	51.6	52.1	51.85	Low	0.1	518.50	4.89E-02	4.89E-02	0.115
FFC12-8b	2	2	14.15	14	49.2	49.1	49.15	Low	0.1	491.50	4.63E-02	4.63E-02	0.12
FFC12-9b	2	2	14.15	14	47.9	48.4	48.15	Low	0.1	481.50	4.54E-02	4.54E-02	0.117

VARIOUS CYCLONE CONFIGURATIONS EXPERIMENT

FILTER NO.	HELIX DESIGN	CYCLONE LENGTH	PARTICLE SIZE (um)	APS PSIZE MEDIAN (um)	FLOW RATE (lpm)	FLUORESCENCE READING CUVET 1	CUVET 2	AVERAGE	PM GAIN	SENSITIVITY RANGE	TRUE READING	CONCENTRATION URANINE (ug/ml)	CORRECTED CONC (ug/ml)	APS CONC (part/cm3)
CYCBLNK3al			0		0	20	24	22.0	Normal	10	2.20	0.000017	-0.000001	
CYCBLNK3aO			0		0	18	28	23.0	Normal	10	2.30	0.000017	0.000001	
CCYC3-1al	2	3	3.58		7	73.5	74.5	74.0	Normal	0.3	246.67	0.001572	0.001554	
CCYC3-1aO	2	3	3.58		7	108	107	107.5	Normal	3	35.83	0.000231	0.000215	
CCYC3-2al	1	2	3.58		7	69.2	69.3	69.3	Normal	0.3	230.83	0.001471	0.001454	
CCYC3-2aO	1	2	3.58		7	76	77.5	76.8	Normal	1	76.75	0.000491	0.000475	
CCYC3-3al	1	3	3.58		7	77.7	77.7	77.7	Normal	0.3	259.00	0.001650	0.001633	
CCYC3-3aO	1	3	3.58		7	43.1	42.8	43.0	Normal	1	42.95	0.000276	0.000260	
CCYC3-4al	2	2	3.58		7	82.8	82.7	82.8	Normal	0.3	275.83	0.001757	0.001740	
CCYC3-4O	2	2	3.58		7	40.2	39.8	40.0	Normal	1	40.00	0.000257	0.000241	
CCYC3-5al	2	1	3.58		7	77.6	77.2	77.4	Normal	0.3	258.00	0.001644	0.001626	
CCYC3-5aO	2	1	3.58		7	53	54	53.5	Normal	1	53.50	0.000343	0.000327	
CCYC3-6al	1	1	3.58		7	77.5	77.4	77.5	Normal	0.3	258.17	0.001645	0.001627	
CCYC3-6aO	1	1	3.58		7	38	38.2	38.1	Normal	1	38.10	0.000245	0.000229	
CCYC3-7al	2	1	3.57		7	75.5	76	75.8	Normal	0.3	252.50	0.001609	0.001591	
CCYC3-7aO	2	1	3.57		7	47	47	47.0	Normal	1	47.00	0.000302	0.000286	
CCYC3-8al	1	2	3.57		7	75.5	75.6	75.6	Normal	0.3	251.83	0.001605	0.001587	
CCYC3-8aO	1	2	3.57		7	56.7	57.3	57.0	Normal	1	57.00	0.000365	0.000349	
CCYC3-9al	1	1	3.57		7	67.9	68	68.0	Normal	0.3	226.50	0.001444	0.001426	
CCYC3-9aO	1	1	3.57		7	41.5	41.9	41.7	Normal	1	41.70	0.000268	0.000252	
CCYC3-10al	2	3	3.57		7	78.2	78.3	78.3	Normal	0.3	260.83	0.001662	0.001644	
CCYC3-10aO	2	3	3.57		7	50.7	50.9	50.8	Normal	1	50.80	0.000326	0.000310	
CCYC3-11al	1	3	3.57		7	73.5	73.2	73.4	Normal	0.3	244.50	0.001558	0.001541	
CCYC3-11aO	1	3	3.57		7	42.7	43.5	43.1	Normal	1	43.10	0.000277	0.000261	
CCYC3-12al	2	2	3.57		7	71.7	71.2	71.5	Normal	0.3	238.17	0.001518	0.001500	
CCYC3-12aO	2	2	3.57		7	86.8	87	86.9	Normal	1	86.90	0.000556	0.000540	
FCBLNK3a2			0	0	0	44	43	43.5	Normal	30	1.45	0.000012	-0.000001	0.000
CFC3-1a	2	3	3.58	3.128	14	52.6	52.9	52.8	Normal	0.1	527.50	0.003358	0.003345	0.502
CFC3-2a	1	2	3.58	3.123	14	50.3	50.7	50.5	Normal	0.1	505.00	0.003215	0.003202	0.532
CFC3-3a	1	3	3.58	3.122	14	51.8	51.9	51.9	Normal	0.1	518.50	0.003301	0.003288	0.535
CFC3-4a	2	2	3.58	3.132	14	48.2	48.3	48.3	Normal	0.1	482.50	0.003072	0.003059	0.516
CFC3-5a	2	1	3.58	3.129	14	52.1	51.8	52.0	Normal	0.1	519.50	0.003307	0.003294	0.532
CFC3-6a	1	1	3.58	3.127	14	54	53.9	54.0	Normal	0.1	539.50	0.003434	0.003421	0.511
CFC3-7a	2	1	3.57	3.106	14	53.7	53.8	53.8	Normal	0.1	537.50	0.003422	0.003409	0.554
CFC3-8a	1	2	3.57	3.11	14	51.1	51.3	51.2	Normal	0.1	512.00	0.003260	0.003246	0.532
CFC3-9a	1	1	3.57	3.116	14	49.6	49.7	49.7	Normal	0.1	496.50	0.003161	0.003148	0.534
CFC3-10a	2	3	3.57	3.112	14	54.8	55	54.9	Normal	0.1	549.00	0.003495	0.003482	0.545

VARIOUS CYCLONE CONFIGURATIONS EXPERIMENT

FILTER NO.	HELIX DESIGN	CYCLONE LENGTH	PARTICLE SIZE (um)	APS PSIZE MEDIAN (um)	FLOW RATE (lpm)	FLUORESCENCE READING CUVET 1	CUVET 2	AVERAGE	PM GAIN	SENSITIVITY RANGE	TRUE READING	CONCENTRATION URANINE (ug/ml)	CORRECTED CONC (ug/ml)	APS CONC (part/cm3)
CFC3-11a	1	3	3.57	3.114	14	55.4	55.2	55.3	Normal	0.1	553.00	0.003520	0.003507	0.529
CFC3-12a	2	2	3.57	3.117	14	52.2	52.2	52.2	Normal	0.1	522.00	0.003323	0.003310	0.531
CYCBLNK6al			0		0	39	44	41.5	Normal	10	4.15	0.000029	0.000012	
CYCBLNK6aO			0		0	18	20	19.0	Normal	10	1.90	0.000015	-0.000001	
CCYC6-1al	2	2	7.04		7	32.9	33.1	33.0	Low	0.3	110.00	0.010408	0.010390	
CCYC6-1aO	2	2	7.04		7	45.5	45.7	45.6	Normal	0.1	456.00	0.002903	0.002887	
CCYC6-2al	1	2	7.04		7	139.7	140.1	139.9	Normal	0.1	1399.00	0.008902	0.008884	
CCYC6-2aO	1	2	7.04		7	65	65.3	65.2	Normal	0.1	651.50	0.004147	0.004131	
CCYC6-3al	2	3	7.04		7	34.1	34.1	34.1	Low	0.3	113.67	0.010753	0.010736	
CCYC6-3aO	2	3	7.04		7	40.3	40.8	40.6	Normal	0.1	405.50	0.002582	0.002566	
CCYC6-4al	1	3	7.04		7	34.3	34	34.2	Low	0.3	113.83	0.010769	0.010751	
CCYC6-4O	1	3	7.04		7	46.9	46.6	46.8	Normal	0.1	467.50	0.002976	0.002961	
CCYC6-5al	1	1	7.04		7	29.1	28.9	29.0	Low	0.3	96.67	0.009152	0.009135	
CCYC6-5aO	1	1	7.04		7	73.4	73	73.2	Normal	0.1	732.00	0.004659	0.004643	
CCYC6-6al	2	1	7.04		7	36.3	36.3	36.3	Low	0.3	121.00	0.011444	0.011426	
CCYC6-6aO	2	1	7.04		7	76.9	77.3	77.1	Normal	0.1	771.00	0.004907	0.004891	
CCYC6-7al	2	3	7.04		7	30.7	30.7	30.7	Low	0.3	102.33	0.009686	0.009668	
CCYC6-7aO	2	3	7.04		7	75.1	74.8	75.0	Normal	0.1	749.50	0.004770	0.004754	
CCYC6-8al	1	2	7.04		7	25.3	25.3	25.3	Low	0.3	84.33	0.007991	0.007973	
CCYC6-8aO	1	2	7.04		7	89.2	89.3	89.3	Normal	0.1	892.50	0.005680	0.005664	
CCYC6-9al	2	1	7.04		7	30.1	30.1	30.1	Low	0.3	100.33	0.009498	0.009480	
CCYC6-9aO	2	1	7.04		7	111.4	111.4	111.4	Normal	0.1	1114.00	0.007089	0.007073	
CCYC6-10al	2	2	7.04		7	32.7	32.9	32.8	Low	0.3	109.33	0.010345	0.010327	
CCYC6-10aO	2	2	7.04		7	83.6	83.4	83.5	Normal	0.1	835.00	0.005314	0.005298	
CCYC6-11al	1	3	7.04		7	38.8	38.9	38.9	Low	0.3	129.50	0.012244	0.012226	
CCYC6-11aO	1	3	7.04		7	39.8	39.9	39.9	Normal	0.1	398.50	0.002538	0.002522	
CCYC6-12al	1	1	7.04		7	22.1	22.2	22.2	Low	0.3	73.83	0.007002	0.006985	
CCYC6-12aO	1	1	7.04		7	109	109.5	109.3	Normal	0.1	1092.50	0.006952	0.006936	
FCBLNK6a2			0	0	0	67	47	57.0	Normal	30	1.90	0.000015	0.000002	0.000
CFC6-1a	2	2	7.04	5.821	14	72.5	72.5	72.5	Low	0.3	241.67	0.022806	0.022793	0.514
CFC6-2a	1	2	7.04	5.824	14	70	70.5	70.3	Low	0.3	234.17	0.022099	0.022086	0.508
CFC6-3a	2	3	7.04	5.819	14	72.6	73.3	73.0	Low	0.3	243.17	0.022947	0.022934	0.497
CFC6-4a	1	3	7.04	5.826	14	73.1	73.2	73.2	Low	0.3	243.83	0.023010	0.022997	0.513
CFC6-5a	1	1	7.04	5.832	14	73.9	73.9	73.9	Low	0.3	246.33	0.023245	0.023232	0.527
CFC6-6a	2	1	7.04	5.826	14	72.8	73	72.9	Low	0.3	243.00	0.022931	0.022918	0.528
CFC6-7a	2	3	7.04	5.782	14	73	72.1	72.6	Low	0.3	241.83	0.022821	0.022808	0.502
CFC6-8a	1	2	7.04	5.808	14	73.1	73.3	73.2	Low	0.3	244.00	0.023025	0.023012	0.513

VARIOUS CYCLONE CONFIGURATIONS EXPERIMENT

FILTER NO.	HELIX DESIGN	CYCLONE LENGTH	PARTICLE SIZE (um)	APS PSIZE MEDIAN (um)	FLOW RATE (lpm)	FLUORESCENCE READING CUVET 1	CUVET 2	AVERAGE	PM GAIN	SENSITIVITY RANGE	TRUE READING	CONCENTRATION URANINE (ug/ml)	CORRECTED CONC (ug/ml)	APS CONC (part/cm3)
CFC6-9a	2	1	7.04	5.82	14	74.2	74.2	74.2	Low	0.3	247.33	0.023339	0.023326	0.518
CFC6-10a	2	2	7.04	5.818	14	75.3	76.2	75.8	Low	0.3	252.50	0.023826	0.023813	0.509
CFC6-11a	1	3	7.04	5.817	14	74.8	74.9	74.9	Low	0.3	249.50	0.023543	0.023530	0.512
CFC6-12a	1	1	7.04	5.819	14	74	74.4	74.2	Low	0.3	247.33	0.023339	0.023326	0.506
CYCBLNK10al			0		0	47	51	49.0	Normal	30	1.63	0.000013	-0.000004	
CYCBLNK10aO			0		0	75	70	72.5	Normal	30	2.42	0.000018	0.000002	
CCYC10-1al	2	1	11.69		7	88.2	88.4	88.3	Low	1	88.30	0.008364	0.008347	
CCYC10-1aO	2	1	11.69		7	40.1	40.4	40.3	Low	1	40.25	0.003840	0.003824	
CCYC10-2al	2	3	11.69		7	98.1	97.9	98.0	Low	1	98.00	0.009278	0.009260	
CCYC10-2aO	2	3	11.69		7	41.6	42.1	41.9	Low	1	41.85	0.003991	0.003975	
CCYC10-3al	1	1	11.69		7	37.4	37.7	37.6	Low	1	37.55	0.003586	0.003568	
CCYC10-3aO	1	1	11.69		7	26.7	26.5	26.6	Low	1	26.60	0.002555	0.002539	
CCYC10-4al	1	2	11.69		7	34.7	34.7	34.7	Low	1	34.70	0.003317	0.003300	
CCYC10-4O	1	2	11.69		7	56.7	56.7	56.7	Normal	0.3	189.00	0.001205	0.001189	
CCYC10-5al	2	2	11.69		7	35.2	35.3	35.3	Low	0.3	117.50	0.011114	0.011096	
CCYC10-5aO	2	2	11.69		7	46.5	46.6	46.6	Normal	0.1	465.50	0.002964	0.002948	
CCYC10-6al	1	3	11.69		7	64.8	65.1	65.0	Normal	0.1	649.50	0.004134	0.004117	
CCYC10-6aO	1	3	11.69		7	83.6	83.8	83.7	Normal	0.3	279.00	0.001777	0.001762	
CCYC10-7al	2	2	11.69		7	95.9	95.6	95.8	Low	1	95.75	0.009066	0.009048	
CCYC10-7aO	2	2	11.69		7	31.7	31.7	31.7	Low	1	31.70	0.003035	0.003019	
CCYC10-8al	2	1	11.69		7	85.6	85.6	85.6	Low	1	85.60	0.008110	0.008093	
CCYC10-8aO	2	1	11.69		7	37.1	37.1	37.1	Low	1	37.10	0.003543	0.003527	
CCYC10-9al	1	3	11.68		7	50	50.3	50.2	Low	1	50.15	0.004772	0.004755	
CCYC10-9aO	1	3	11.68		7	81.4	81	81.2	Normal	0.3	270.67	0.001724	0.001709	
CCYC10-10al	2	3	11.68		7	92.2	91.8	92.0	Low	1	92.00	0.008713	0.008695	
CCYC10-10aO	2	3	11.68		7	66.1	66	66.1	Normal	0.1	660.50	0.004204	0.004188	
CCYC10-11al	1	1	11.68		7	60.4	60.5	60.5	Normal	0.1	604.50	0.003848	0.003830	
CCYC10-11aO	1	1	11.68		7	36.6	36.5	36.6	Normal	0.1	365.50	0.002328	0.002312	
CCYC10-12al	1	2	11.68		7	51.7	51.8	51.8	Normal	0.1	517.50	0.003295	0.003277	
CCYC10-12aO	1	2	11.68		7	83.5	83.7	83.6	Normal	0.3	278.67	0.001775	0.001759	
FCBLNK10a2			0	0	0	62	49	55.5	Normal	30	1.85	0.000015	0.000001	0.000
CFC10-1a	2	1	11.69	9.399	14	39.2	39.1	39.2	Low	0.1	391.50	0.036914	0.036901	0.205
CFC10-2a	2	3	11.69	9.432	14	36.7	37	36.9	Low	0.1	368.50	0.034748	0.034735	0.185
CFC10-3a	1	1	11.69	9.475	14	39.4	39.3	39.4	Low	0.1	393.50	0.037103	0.037089	0.185
CFC10-4a	1	2	11.69	9.488	14	40	39.9	40.0	Low	0.1	399.50	0.037668	0.037654	0.190
CFC10-5a	2	2	11.69	9.454	14	39	38.8	38.9	Low	0.1	389.00	0.036679	0.036666	0.188
CFC10-6a	1	3	11.69	9.455	14	40.1	40.2	40.2	Low	0.1	401.50	0.037856	0.037843	0.182

VARIOUS CYCLONE CONFIGURATIONS EXPERIMENT

FILTER NO.	HELIX DESIGN	CYCLONE LENGTH	PARTICLE SIZE (um)	APS PSIZE MEDIAN (um)	FLOW RATE (lpm)	FLUORESCENCE READING CUVET 1	CUVET 2	AVERAGE	PM GAIN	SENSITIVITY RANGE	TRUE READING	CONCENTRATION URANINE (ug/ml)	CORRECTED CONC (ug/ml)	APS CONC (part/cm3)
CFC10-7a	2	2	11.68	9.454	14	39.8	39.7	39.8	Low	0.1	397.50	0.037479	0.037466	0.188
CFC10-8a	2	1	11.68	9.455	14	39	39.2	39.1	Low	0.1	391.00	0.036867	0.036854	0.192
CFC10-9a	1	3	11.68	9.458	14	38.7	38.9	38.8	Low	0.1	388.00	0.036585	0.036571	0.184
CFC10-10a	2	3	11.68	9.465	14	38.7	39.1	38.9	Low	0.1	389.00	0.036679	0.036666	0.182
CFC10-11a	1	1	11.68	9.442	14	38.8	38.7	38.8	Low	0.1	387.50	0.036538	0.036524	0.181
CFC10-12a	1	2	11.68	9.467	14	38.8	38.6	38.7	Low	0.1	387.00	0.036490	0.036477	0.187
CYCBLNK8al			0		0	56	50	53.0	Normal	30	1.77	0.000014	-0.000003	
CYCBLNK8aO			0		0	50	50	50.0	Normal	30	1.67	0.000013	-0.000003	
CCYC8-1al	1	1	9.39		7	84	84.1	84.1	Normal	0.1	840.50	0.005349	0.005332	
CCYC8-1aO	1	1	9.39		7	35	35	35.0	Normal	0.1	350.00	0.002229	0.002213	
CCYC8-2al	1	3	9.39		7	99.8	100.6	100.2	Normal	0.1	1002.00	0.006376	0.006359	
CCYC8-2aO	1	3	9.39		7	40.5	40.7	40.6	Normal	0.1	406.00	0.002585	0.002569	
CCYC8-3al	2	2	9.39		7	90.8	91.1	91.0	Low	1	90.95	0.008614	0.008596	
CCYC8-3aO	2	2	9.39		7	48.8	49.4	49.1	Normal	0.1	491.00	0.003126	0.003110	
CCYC8-4al	1	2	9.39		7	77.1	77.1	77.1	Normal	0.1	771.00	0.004907	0.004890	
CCYC8-4O	1	2	9.39		7	89.1	89.4	89.3	Normal	0.3	297.50	0.001895	0.001879	
CCYC8-5al	2	1	9.39		7	92.3	92.1	92.2	Low	1	92.20	0.008732	0.008714	
CCYC8-5aO	2	1	9.39		7	51	51.2	51.1	Normal	0.1	511.00	0.003253	0.003237	
CCYC8-6al	2	3	9.39		7	89.1	89.4	89.3	Low	1	89.25	0.008454	0.008436	
CCYC8-6aO	2	3	9.39		7	54.9	55.2	55.1	Normal	0.1	550.50	0.003504	0.003489	
CCYC8-7al	1	1	9.37		7	81.9	81.4	81.7	Normal	0.1	816.50	0.005196	0.005179	
CCYC8-7aO	1	1	9.37		7	31.1	31.2	31.2	Normal	0.1	311.50	0.001984	0.001968	
CCYC8-8al	2	3	9.37		7	105.1	105.2	105.2	Low	1	105.15	0.009951	0.009934	
CCYC8-8aO	2	3	9.37		7	48.4	48.8	48.6	Normal	0.1	486.00	0.003094	0.003078	
CCYC8-9al	1	2	9.37		7	93.7	93.7	93.7	Normal	0.1	937.00	0.005963	0.005945	
CCYC8-9aO	1	2	9.37		7	78.7	78	78.4	Normal	0.3	261.17	0.001664	0.001648	
CCYC8-10al	2	1	9.37		7	93.6	93.7	93.7	Low	1	93.65	0.008868	0.008851	
CCYC8-10aO	2	1	9.37		7	44	44.1	44.1	Normal	0.1	440.50	0.002805	0.002789	
CCYC8-11al	2	2	9.37		7	93	93.3	93.2	Low	1	93.15	0.008821	0.008804	
CCYC8-11aO	2	2	9.37		7	47.4	47.3	47.4	Normal	0.1	473.50	0.003015	0.002999	
CCYC8-12al	1	3	9.37		7	90.1	90.3	90.2	Normal	0.1	902.00	0.005740	0.005723	
CCYC8-12aO	1	3	9.37		7	62.6	62.6	62.6	Normal	0.3	208.67	0.001330	0.001314	
FCBLNK8a2			0	0	0	44	48	46.0	Normal	30	1.53	0.000013	-0.000001	0.000
CFC8-1a	1	1	9.39	8.276	14	88.5	88.8	88.7	Low	0.3	295.50	0.027875	0.027862	0.228
CFC8-2a	1	3	9.39	8.266	14	89.2	89.6	89.4	Low	0.3	298.00	0.028110	0.028097	0.226
CFC8-3a	2	2	9.39	8.233	14	86.9	87.5	87.2	Low	0.3	290.67	0.027420	0.027406	0.235
CFC8-4a	1	2	9.39	8.242	14	89.6	90.3	90.0	Low	0.3	299.83	0.028283	0.028270	0.227

VARIOUS CYCLONE CONFIGURATIONS EXPERIMENT

FILTER NO.	HELIX DESIGN	CYCLONE LENGTH	PARTICLE SIZE (um)	APS PSIZE MEDIAN (um)	FLOW RATE (lpm)	FLUORESCENCE READING CUVET 1	CUVET 2	AVERAGE	PM GAIN	SENSITIVITY RANGE	TRUE READING	CONCENTRATION URANINE (ug/ml)	CORRECTED CONC (ug/ml)	APS CONC (part/cm3)
CFC8-5a	2	1	9.39	8.212	14	87.9	88.2	88.1	Low	0.3	293.50	0.027686	0.027673	0.228
CFC8-6a	2	3	9.39	8.251	14	88.4	88.7	88.6	Low	0.3	295.17	0.027843	0.027830	0.222
CFC8-7a	1	1	9.37	8.192	14	90.1	90.4	90.3	Low	0.3	300.83	0.028377	0.028364	0.220
CFC8-8a	2	3	9.37	8.204	14	91.1	90.9	91.0	Low	0.3	303.33	0.028612	0.028599	0.224
CFC8-9a	1	2	9.37	8.266	14	91.2	92.5	91.9	Low	0.3	306.17	0.028879	0.028866	0.225
CFC8-10a	2	1	9.37	8.242	14	90.8	90.7	90.8	Low	0.3	302.50	0.028534	0.028521	0.228
CFC8-11a	2	2	9.37	8.239	14	90.9	90.9	90.9	Low	0.3	303.00	0.028581	0.028568	0.229
CFC8-12a	1	3	9.37	8.254	14	92.4	92.1	92.3	Low	0.3	307.50	0.029005	0.028991	0.223
CYCBLNK45al			0		0	92	115	103.5	Normal	30	3.45	0.000025	0.000007	
CYCBLNK45aO			0		0	77	84	80.5	Normal	30	2.68	0.000020	0.000004	
CCYC45-1al	2	2	5.28		7	72.5	73.3	72.9	Normal	0.1	729.00	0.004640	0.004622	
CCYC45-1aO	2	2	5.28		7	42.2	42.6	42.4	Normal	0.1	424.00	0.002700	0.002684	
CCYC45-2al	1	2	5.28		7	59.4	59.9	59.7	Normal	0.1	596.50	0.003797	0.003780	
CCYC45-2aO	1	2	5.28		7	24.4	24.4	24.4	Normal	0.1	244.00	0.001555	0.001539	
CCYC45-3al	2	3	5.28		7	82.2	83.1	82.7	Low	1	82.65	0.007832	0.007815	
CCYC45-3aO	2	3	5.28		7	19.5	19.5	19.5	Normal	0.1	195.00	0.001243	0.001227	
CCYC45-4al	2	1	5.28		7	83.8	83.4	83.6	Normal	0.1	836.00	0.005320	0.005303	
CCYC45-4O	2	1	5.28		7	20.4	20.4	20.4	Normal	0.3	68.00	0.000435	0.000419	
CCYC45-5al	1	3	5.28		7	92.5	93	92.8	Low	1	92.75	0.008783	0.008766	
CCYC45-5aO	1	3	5.28		7	14.1	14.1	14.1	Normal	0.1	141.00	0.000900	0.000884	
CCYC45-6al	1	1	5.28		7	75.7	75.8	75.8	Low	1	75.75	0.007183	0.007165	
CCYC45-6aO	1	1	5.28		7	23.4	23.7	23.6	Normal	0.1	235.50	0.001501	0.001485	
CCYC45-7al	2	1	5.24		7	91.1	90.7	90.9	Normal	0.1	909.00	0.005785	0.005767	
CCYC45-7aO	2	1	5.24		7	18.6	18.6	18.6	Normal	0.1	186.00	0.001186	0.001170	
CCYC45-8al	2	2	5.24		7	92.3	91.6	92.0	Low	1	91.95	0.008708	0.008691	
CCYC45-8aO	2	2	5.24		7	15.5	15.6	15.6	Normal	0.1	155.50	0.000992	0.000976	
CCYC45-9al	1	3	5.24		7	83	83	83.0	Normal	0.1	830.00	0.005282	0.005265	
CCYC45-9aO	1	3	5.24		7	16.2	16.1	16.2	Normal	0.3	53.83	0.000345	0.000329	
CCYC45-10al	1	1	5.24		7	77.1	77.3	77.2	Low	1	77.20	0.007319	0.007302	
CCYC45-10aO	1	1	5.24		7	19	19	19.0	Normal	0.1	190.00	0.001211	0.001195	
CCYC45-11al	1	2	5.24		7	85.7	85.9	85.8	Low	1	85.80	0.008129	0.008112	
CCYC45-11aO	1	2	5.24		7	16.1	16	16.1	Normal	0.1	160.50	0.001024	0.001008	
CCYC45-12al	2	3	5.24		7	93	92.7	92.9	Normal	0.1	928.50	0.005909	0.005891	
CCYC45-12aO	2	3	5.24		7	15.3	15.3	15.3	Normal	0.3	51.00	0.000327	0.000311	
FCBLNK45a2			0	0	0	46	33	39.5	Normal	30	1.32	0.000011	-0.000002	0.000
CFC45-1a	2	2	5.28	4.687	14	34.2	34.4	34.3	Low	0.3	114.33	0.010816	0.010803	0.479
CFC45-2a	1	2	5.28	4.685	14	33.2	32.9	33.1	Low	0.3	110.17	0.010423	0.010410	0.486

VARIOUS CYCLONE CONFIGURATIONS EXPERIMENT

FILTER NO.	HELIX DESIGN	CYCLONE LENGTH	PARTICLE SIZE (um)	APS PSIZE MEDIAN (um)	FLOW RATE (lpm)	FLUORESCENCE READING CUVET 1	CUVET 2	AVERAGE	PM GAIN	SENSITIVITY RANGE	TRUE READING	CONCENTRATION URANINE (ug/ml)	CORRECTED CONC (ug/ml)	APS CONC (part/cm3)
CFC45-3a	2	3	5.28	4.677	14	33	33	33.0	Low	0.3	110.00	0.010408	0.010395	0.484
CFC45-4a	2	1	5.28	4.679	14	34	33.9	34.0	Low	0.3	113.17	0.010706	0.010693	0.484
CFC45-5a	1	3	5.28	4.683	14	33.7	33.6	33.7	Low	0.3	112.17	0.010612	0.010599	0.495
CFC45-6a	1	1	5.28	4.68	14	32.8	33.1	33.0	Low	0.3	109.83	0.010392	0.010379	0.482
CFC45-7a	2	1	5.24	4.613	14	31.7	31.7	31.7	Low	0.3	105.67	0.010000	0.009987	0.502
CFC45-8a	2	2	5.24	4.64	14	32.6	32.6	32.6	Low	0.3	108.67	0.010282	0.010269	0.524
CFC45-9a	1	3	5.24	4.627	14	32.9	33	33.0	Low	0.3	109.83	0.010392	0.010379	0.513
CFC45-10a	1	1	5.24	4.634	14	32.6	33	32.8	Low	0.3	109.33	0.010345	0.010332	0.526
CFC45-11a	1	2	5.24	4.638	14	32.9	32.9	32.9	Low	0.3	109.67	0.010376	0.010363	0.522
CFC45-12a	2	3	5.24	4.637	14	32.8	33	32.9	Low	0.3	109.67	0.010376	0.010363	0.515
CYCBLNK8bI			0		0	56	51	53.5	Normal	30	1.78	0.000014	-0.000003	
CYCBLNK8bO			0		0	39	70	54.5	Normal	30	1.82	0.000014	-0.000002	
CCYC8-1bI	1	1	9.27		7	106.3	107.2	106.8	Normal	0.1	1067.50	0.006793	0.006775	
CCYC8-1bO	1	1	9.27		7	57.6	57.8	57.7	Normal	0.1	577.00	0.003673	0.003657	
CCYC8-2bI	1	2	9.27		7	133.2	132.7	133.0	Normal	0.1	1329.50	0.008460	0.008442	
CCYC8-2bO	1	2	9.27		7	35.3	35.5	35.4	Normal	0.1	354.00	0.002255	0.002239	
CCYC8-3bI	2	3	9.27		7	113.9	114.2	114.1	Low	1	114.05	0.010789	0.010772	
CCYC8-3bO	2	3	9.27		7	35.8	35.7	35.8	Normal	0.1	357.50	0.002277	0.002261	
CCYC8-4bI	2	2	9.27		7	107.2	107.1	107.2	Low	1	107.15	0.010139	0.010122	
CCYC8-4O	2	2	9.27		7	43.2	43.1	43.2	Normal	0.1	431.50	0.002748	0.002732	
CCYC8-5bI	2	1	9.27		7	115	114.2	114.6	Low	1	114.60	0.010841	0.010823	
CCYC8-5bO	2	1	9.27		7	61.3	61.2	61.3	Normal	0.1	612.50	0.003899	0.003883	
CCYC8-6bI	1	3	9.27		7	126.2	125.6	125.9	Normal	0.1	1259.00	0.008011	0.007994	
CCYC8-6bO	1	3	9.27		7	31.8	31.8	31.8	Normal	0.1	318.00	0.002026	0.002010	
CCYC8-7bI	1	3	9.19		7	137	137.4	137.2	Normal	0.1	1372.00	0.008730	0.008712	
CCYC8-7bO	1	3	9.19		7	28.1	28.2	28.2	Normal	0.1	281.50	0.001793	0.001777	
CCYC8-8bI	1	1	9.19		7	110.4	110.9	110.7	Normal	0.1	1106.50	0.007041	0.007024	
CCYC8-8bO	1	1	9.19		7	52.3	52.8	52.6	Normal	0.1	525.50	0.003345	0.003329	
CCYC8-9bI	2	2	9.19		7	110.4	110.2	110.3	Low	1	110.30	0.010436	0.010419	
CCYC8-9bO	2	2	9.19		7	53	54	53.5	Normal	0.1	535.00	0.003406	0.003390	
CCYC8-10bI	2	1	9.19		7	109.3	108.8	109.1	Low	1	109.05	0.010318	0.010301	
CCYC8-10bO	2	1	9.19		7	61	61.2	61.1	Normal	0.1	611.00	0.003889	0.003873	
CCYC8-11bI	2	3	9.19		7	121.4	121.5	121.5	Low	1	121.45	0.011486	0.011468	
CCYC8-11bO	2	3	9.19		7	50.1	50.2	50.2	Normal	0.1	501.50	0.003193	0.003177	
CCYC8-12bI	1	2	9.19		7	89	89	89.0	Low	1	89.00	0.008430	0.008413	
CCYC8-12bO	1	2	9.19		7	36.2	36.7	36.5	Normal	0.1	364.50	0.002321	0.002305	
FCBLNK8b2			0	0	0	70	69	69.5	Normal	30	2.32	0.000018	0.000004	0.000

VARIOUS CYCLONE CONFIGURATIONS EXPERIMENT

FILTER NO.	HELIX DESIGN	CYCLONE LENGTH	PARTICLE SIZE (um)	APS PSIZE MEDIAN (um)	FLOW RATE (lpm)	FLUORESCENCE READING CUVET 1	CUVET 2	AVERAGE	PM GAIN	SENSITIVITY RANGE	TRUE READING	CONCENTRATION URANINE (ug/ml)	CORRECTED CONC (ug/ml)	APS CONC (part/cm3)
CFC8-1b	1	1	9.27	7.62	14	85.3	86	85.7	Low	0.3	285.50	0.026933	0.026920	0.286
CFC8-2b	1	2	9.27	7.603	14	84.8	85.3	85.1	Low	0.3	283.50	0.026745	0.026732	0.294
CFC8-3b	2	3	9.27	7.607	14	84.9	85.1	85.0	Low	0.3	283.33	0.026729	0.026716	0.300
CFC8-4b	2	2	9.27	7.606	14	86.9	87.7	87.3	Low	0.3	291.00	0.027451	0.027438	0.294
CFC8-5b	2	1	9.27	7.6	14	86.5	87	86.8	Low	0.3	289.17	0.027278	0.027265	0.297
CFC8-6b	1	3	9.27	7.625	14	86.7	87.6	87.2	Low	0.3	290.50	0.027404	0.027391	0.288
CFC8-7b	1	3	9.19	7.7	14	89.2	88.8	89.0	Low	0.3	296.67	0.027985	0.027971	0.291
CFC8-8b	1	1	9.19	7.707	14	89.4	89.4	89.4	Low	0.3	298.00	0.028110	0.028097	0.292
CFC8-9b	2	2	9.19	7.713	14	90.7	90.6	90.7	Low	0.3	302.17	0.028502	0.028489	0.300
CFC8-10b	2	1	9.19	7.685	14	90.8	90.5	90.7	Low	0.3	302.17	0.028502	0.028489	0.306
CFC8-11b	2	3	9.19	7.704	14	91.5	91.6	91.6	Low	0.3	305.17	0.028785	0.028772	0.297
CFC8-12b	1	2	9.19	7.681	14	90.8	91.1	91.0	Low	0.3	303.17	0.028597	0.028583	0.311
CYCBLNK6bI			0		0	63	47	55.0	Normal	30	1.83	0.000014	-0.000003	
CYCBLNK6bO			0		0	49	59	54.0	Normal	30	1.80	0.000014	-0.000002	
CCYC6-1bI	1	1	7.02		7	102.7	102.4	102.6	Low	1	102.55	0.009706	0.009689	
CCYC6-1bO	1	1	7.02		7	61.3	61.5	61.4	Normal	0.3	204.67	0.001305	0.001289	
CCYC6-2bI	1	3	7.02		7	100.3	99.9	100.1	Low	1	100.10	0.009476	0.009458	
CCYC6-2bO	1	3	7.02		7	113.2	113	113.1	Normal	0.3	377.00	0.002401	0.002385	
CCYC6-3bI	2	1	7.02		7	109.1	108.6	108.9	Low	1	108.85	0.010299	0.010282	
CCYC6-3bO	2	1	7.02		7	130.2	131.2	130.7	Normal	0.3	435.67	0.002774	0.002758	
CCYC6-4bI	2	2	7.02		7	82.9	83.1	83.0	Low	1	83.00	0.007865	0.007848	
CCYC6-4O	2	2	7.02		7	115.2	115.8	115.5	Normal	0.3	385.00	0.002452	0.002436	
CCYC6-5bI	2	3	7.02		7	116.4	116	116.2	Low	1	116.20	0.010992	0.010974	
CCYC6-5bO	2	3	7.02		7	124.6	125.1	124.9	Normal	0.3	416.17	0.002650	0.002634	
CCYC6-6bI	1	2	7.02		7	99.7	99.8	99.8	Low	1	99.75	0.009443	0.009425	
CCYC6-6bO	1	2	7.02		7	124.8	125.7	125.3	Normal	0.3	417.50	0.002658	0.002643	
CCYC6-7bI	2	3	7.01		7	124.7	124.8	124.8	Low	1	124.75	0.011797	0.011779	
CCYC6-7bO	2	3	7.01		7	111.4	111.4	111.4	Normal	0.3	371.33	0.002365	0.002349	
CCYC6-8bI	2	1	7.01		7	118.5	118.1	118.3	Low	1	118.30	0.011189	0.011172	
CCYC6-8bO	2	1	7.01		7	52.2	52.8	52.5	Normal	0.1	525.00	0.003342	0.003326	
CCYC6-9bI	1	2	7.01		7	102.8	101.9	102.4	Low	1	102.35	0.009687	0.009670	
CCYC6-9bO	1	2	7.01		7	46.6	46.5	46.6	Normal	0.1	465.50	0.002964	0.002948	
CCYC6-10bI	1	1	7.01		7	94.7	95.5	95.1	Low	1	95.10	0.009005	0.008987	
CCYC6-10bO	1	1	7.01		7	44.3	44.2	44.3	Normal	0.1	442.50	0.002817	0.002802	
CCYC6-11bI	2	2	7.01		7	128.8	129.4	129.1	Low	1	129.10	0.012206	0.012189	
CCYC6-11bO	2	2	7.01		7	37.6	37.1	37.4	Normal	0.1	373.50	0.002379	0.002363	
CCYC6-12bI	1	3	7.01		7	104.4	103.8	104.1	Low	1	104.10	0.009852	0.009835	

VARIOUS CYCLONE CONFIGURATIONS EXPERIMENT

FILTER NO.	HELIX DESIGN	CYCLONE LENGTH	PARTICLE SIZE (um)	APS PSIZE MEDIAN (um)	FLOW RATE (lpm)	FLUORESCENCE READING CUVET 1	CUVET 2	AVERAGE	PM GAIN	SENSITIVITY RANGE	TRUE READING	CONCENTRATION URANINE (ug/ml)	CORRECTED CONC (ug/ml)	APS CONC (part/cm3)
CCYC6-12bO	1	3	7.01		7	50.1	50.2	50.2	Normal	0.1	501.50	0.003193	0.003177	
FCBLNK6b2			0	0	0	67	68	67.5	Normal	30	2.25	0.000017	0.000004	0.000
CFC6-1b	1	1	7.02	5.947	14	69.4	69.4	69.4	Low	0.3	231.33	0.021833	0.021820	0.452
CFC6-2b	1	3	7.02	5.946	14	70.7	71.2	71.0	Low	0.3	236.50	0.022319	0.022306	0.465
CFC6-3b	2	1	7.02	5.932	14	71.4	71.4	71.4	Low	0.3	238.00	0.022460	0.022447	0.468
CFC6-4b	2	2	7.02	5.936	14	71.2	71.7	71.5	Low	0.3	238.17	0.022476	0.022463	0.490
CFC6-5b	2	3	7.02	5.939	14	72.6	72.3	72.5	Low	0.3	241.50	0.022790	0.022777	0.460
CFC6-6b	1	2	7.02	5.937	14	71.8	72.4	72.1	Low	0.3	240.33	0.022680	0.022667	0.467
CFC6-7b	2	3	7.01	5.924	14	70.9	71.5	71.2	Low	0.3	237.33	0.022398	0.022384	0.464
CFC6-8b	2	1	7.01	5.928	14	73.4	73.1	73.3	Low	0.3	244.17	0.023041	0.023028	0.478
CFC6-9b	1	2	7.01	5.936	14	73.8	73.6	73.7	Low	0.3	245.67	0.023182	0.023169	0.485
CFC6-10b	1	1	7.01	5.944	14	74.7	74.8	74.8	Low	0.3	249.17	0.023512	0.023499	0.475
CFC6-11b	2	2	7.01	5.947	14	73.8	74.9	74.4	Low	0.3	247.83	0.023386	0.023373	0.490
CFC6-12b	1	3	7.01	5.938	14	75	75.7	75.4	Low	0.3	251.17	0.023700	0.023687	0.465
CYCBLNK3bI			0		0	51	77	64.0	Normal	30	2.13	0.000016	-0.000001	
CYCBLNK3bO			0		0	76	69	72.5	Normal	30	2.42	0.000018	0.000002	
CCYC3-1bI	2	1	3.56		7	52.7	52.9	52.8	Normal	0.3	176.00	0.001122	0.001105	
CCYC3-1bO	2	1	3.56		7	37.7	38.2	38.0	Normal	1	37.95	0.000244	0.000228	
CCYC3-2bI	2	3	3.56		7	51.1	51.2	51.2	Normal	0.3	170.50	0.001087	0.001070	
CCYC3-2bO	2	3	3.56		7	38.6	39	38.8	Normal	1	38.60	0.000250	0.000234	
CCYC3-3bI	2	2	3.56		7	47.2	47.2	47.2	Normal	0.3	157.33	0.001004	0.000988	
CCYC3-3bO	2	2	3.56		7	47.5	47.9	47.7	Normal	1	47.70	0.000306	0.000290	
CCYC3-4bI	1	2	3.56		7	51.4	51.4	51.4	Normal	0.3	171.33	0.001093	0.001075	
CCYC3-4O	1	2	3.56		7	29.6	29.2	29.4	Normal	1	29.40	0.000190	0.000174	
CCYC3-5bI	1	1	3.56		7	51	50.8	50.9	Normal	0.3	169.67	0.001082	0.001065	
CCYC3-5bO	1	1	3.56		7	35.5	35.4	35.5	Normal	1	35.45	0.000228	0.000212	
CCYC3-6bI	1	3	3.56		7	48.6	49.1	48.9	Normal	0.3	162.83	0.001039	0.001021	
CCYC3-6bO	1	3	3.56		7	32	32.1	32.1	Normal	1	32.05	0.000207	0.000191	
CCYC3-7bI	2	2	3.55		7	48	48.3	48.2	Normal	0.3	160.50	0.001024	0.001006	
CCYC3-7bO	2	2	3.55		7	51.1	50.4	50.8	Normal	1	50.75	0.000326	0.000310	
CCYC3-8bI	1	2	3.55		7	50.8	50.1	50.5	Normal	0.3	168.17	0.001072	0.001055	
CCYC3-8bO	1	2	3.55		7	36.3	36.3	36.3	Normal	1	36.30	0.000234	0.000218	
CCYC3-9bI	2	3	3.55		7	53.5	53.5	53.5	Normal	0.3	178.33	0.001137	0.001120	
CCYC3-9bO	2	3	3.55		7	39.9	39.8	39.9	Normal	1	39.65	0.000256	0.000240	
CCYC3-10bI	1	1	3.55		7	49.4	49.3	49.4	Normal	0.3	164.50	0.001049	0.001032	
CCYC3-10bO	1	1	3.55		7	37.9	37.5	37.7	Normal	1	37.70	0.000243	0.000227	
CCYC3-11bI	1	3	3.55		7	49.5	49.8	49.7	Normal	0.3	165.50	0.001056	0.001038	

VARIOUS CYCLONE CONFIGURATIONS EXPERIMENT

FILTER NO.	HELIX DESIGN	CYCLONE LENGTH	PARTICLE SIZE (um)	APS PSIZE MEDIAN (um)	FLOW RATE (lpm)	FLUORESCENCE READING CUVET 1	CUVET 2	AVERAGE	PM GAIN	SENSITIVITY RANGE	TRUE READING	CONCENTRATION URANINE (ug/ml)	CORRECTED CONC (ug/ml)	APS CONC (part/cm3)
CCYC3-11bO	1	3	3.55		7	37.7	38.8	38.3	Normal	1	38.25	0.000246	0.000230	
CCYC3-12bI	2	1	3.55		7	57.9	57.4	57.7	Normal	0.3	192.17	0.001225	0.001208	
CCYC3-12bO	2	1	3.55		7	35.2	35.7	35.5	Normal	1	35.45	0.000228	0.000212	
FCBLNK3b2			0	0	0	48	37	42.5	Normal	30	1.42	0.000012	-0.000001	0.000
CFC3-1b	2	1	3.56	2.784	14	94.3	94.7	94.5	Normal	0.3	315.00	0.002006	0.001993	0.463
CFC3-2b	2	3	3.56	2.794	14	102.6	103.7	103.2	Normal	0.3	343.83	0.002190	0.002177	0.436
CFC3-3b	2	2	3.56	2.796	14	94.2	95.1	94.7	Normal	0.3	315.50	0.002010	0.001996	0.451
CFC3-4b	1	2	3.56	2.793	14	100.3	99.8	100.1	Normal	0.3	333.50	0.002124	0.002111	0.454
CFC3-5b	1	1	3.56	2.795	14	104.5	104.4	104.5	Normal	0.3	348.17	0.002217	0.002204	0.454
CFC3-6b	1	3	3.56		14	107.5	107.3	107.4	Normal	0.3	358.00	0.002280	0.002267	
CFC3-7b	2	2	3.55	2.805	14	88.8	89.1	89.0	Normal	0.3	296.50	0.001889	0.001876	0.454
CFC3-8b	1	2	3.55	2.81	14	105.8	106	105.9	Normal	0.3	353.00	0.002248	0.002235	0.445
CFC3-9b	2	3	3.55	2.81	14	108.4	108.6	108.5	Normal	0.3	361.67	0.002303	0.002290	0.450
CFC3-10b	1	1	3.55	2.81	14	110.7	110.7	110.7	Normal	0.3	369.00	0.002350	0.002337	0.453
CFC3-11b	1	3	3.55	2.819	14	108.1	108.7	108.4	Normal	0.3	361.33	0.002301	0.002288	0.449
CFC3-12b	2	1	3.55	2.819	14	113.3	112.6	113.0	Normal	0.3	376.50	0.002398	0.002384	0.445
CYCBLNK10bI			0		0	47	68	57.5	Normal	30	1.92	0.000015	-0.000003	
CYCBLNK10bO			0		0	75	42	58.5	Normal	30	1.95	0.000015	-0.000001	
CCYC10-1bI	2	1	11.79		7	114.6	114.8	114.7	Normal	0.1	1148.00	0.007305	0.007288	
CCYC10-1bO	2	1	11.79		7	52.6	53.1	52.9	Normal	0.1	531.00	0.003380	0.003364	
CCYC10-2bI	1	1	11.79		7	56.8	56.9	56.9	Normal	0.1	569.00	0.003622	0.003605	
CCYC10-2bO	1	1	11.79		7	19.3	19.6	19.5	Normal	0.1	196.00	0.001250	0.001234	
CCYC10-3bI	2	2	11.79		7	95.7	97.1	96.4	Low	1	97.10	0.009193	0.009176	
CCYC10-3bO	2	2	11.79		7	22.7	22.9	22.8	Normal	0.1	229.00	0.001459	0.001443	
CCYC10-4bI	1	3	11.79		7	81.2	81.3	81.3	Normal	0.1	813.00	0.005174	0.005157	
CCYC10-4O	1	3	11.79		7	22.7	22.6	22.7	Normal	0.1	226.00	0.001440	0.001424	
CCYC10-5bI	2	3	11.79		7	130.3	130.4	130.4	Normal	0.1	1304.00	0.008297	0.008280	
CCYC10-5bO	2	3	11.79		7	38.1	38.2	38.2	Normal	0.1	382.00	0.002433	0.002417	
CCYC10-6bI	1	2	11.79		7	91.5	91.8	91.7	Normal	0.1	918.00	0.005842	0.005825	
CCYC10-6bO	1	2	11.79		7	31.8	31.7	31.8	Normal	0.1	317.00	0.002019	0.002003	
CCYC10-7bI	1	3	11.79		7	61.1	60.9	61.0	Normal	0.1	609.00	0.003877	0.003859	
CCYC10-7bO	1	3	11.79		7	39.8	39.6	39.7	Normal	0.3	132.00	0.000842	0.000826	
CCYC10-8bI	2	1	11.79		7	114	114.6	114.3	Normal	0.1	1146.00	0.007292	0.007275	
CCYC10-8bO	2	1	11.79		7	66.6	66.8	66.7	Normal	0.1	667.00	0.004245	0.004230	
CCYC10-9bI	1	2	11.79		7	71.2	71.4	71.3	Normal	0.1	713.00	0.004538	0.004521	
CCYC10-9bO	1	2	11.79		7	22.3	22.1	22.2	Normal	0.1	222.00	0.001415	0.001399	
CCYC10-10bI	2	3	11.79		7	107.1	106.1	106.6	Low	1	106.60	0.010088	0.010070	

VARIOUS CYCLONE CONFIGURATIONS EXPERIMENT

FILTER NO.	HELIX DESIGN	CYCLONE LENGTH	PARTICLE SIZE (um)	APS PSIZE MEDIAN (um)	FLOW RATE (lpm)	FLUORESCENCE READING CUVET 1	CUVET 2	AVERAGE	PM GAIN	SENSITIVITY RANGE	TRUE READING	CONCENTRATION URANINE (ug/ml)	CORRECTED CONC (ug/ml)	APS CONC (part/cm3)
CCYC10-10b	2	3	11.79		7	45.3	45.5	45.4	Normal	0.1	454.00	0.002891	0.002875	
CCYC10-11bl	2	2	11.79		7	111.6	110.1	110.9	Low	1	110.85	0.010488	0.010470	
CCYC10-11b	2	2	11.79		7	50.2	50.2	50.2	Normal	0.1	502.00	0.003196	0.003180	
CCYC10-12bl	1	1	11.79		7	61.7	61.7	61.7	Normal	0.1	617.00	0.003927	0.003910	
CCYC10-12b	1	1	11.79		7	24.7	24.8	24.8	Normal	0.1	247.50	0.001577	0.001561	
FCBLNK10b2			0	0	0	45	33	39.0	Normal	30	1.30	0.000011	-0.000002	0.000
CFC10-1b	2	1	11.79	9.124	14	108.5	108.4	108.5	Low	0.3	361.50	0.034089	0.034076	0.192
CFC10-2b	1	1	11.79	9.135	14	108.7	107.3	108.0	Low	0.3	360.00	0.033948	0.033935	0.187
CFC10-3b	2	2	11.79	9.154	14	102.8	103.2	103.0	Low	0.3	343.33	0.032379	0.032366	0.175
CFC10-4b	1	3	11.79	9.105	14	112.1	112.2	112.2	Low	0.3	373.83	0.035251	0.035238	0.205
CFC10-5b	2	3	11.79	9.106	14	112.5	113.1	112.8	Low	0.3	376.00	0.035455	0.035442	0.216
CFC10-6b	1	2	11.79	9.112	14	113.7	114.8	114.3	Low	0.3	380.83	0.035910	0.035897	0.205
CFC10-7b	1	3	11.79	9.105	14	104	104.7	104.4	Low	0.3	347.83	0.032802	0.032789	0.199
CFC10-8b	2	1	11.79	9.108	14	104.3	104.8	104.6	Low	0.3	348.50	0.032865	0.032852	0.168
CFC10-9b	1	2	11.79	9.103	14	106.6	106.9	106.8	Low	0.3	355.83	0.033556	0.033543	0.197
CFC10-10b	2	3	11.79	9.106	14	106.9	106.4	106.7	Low	0.3	355.50	0.033524	0.033511	0.198
CFC10-11b	2	2	11.79	9.094	14	107.8	107.5	107.7	Low	0.3	358.83	0.033838	0.033825	0.202
CFC10-12b	1	1	11.79	9.103	14	109.8	109.2	109.5	Low	0.3	365.00	0.034419	0.034406	0.198
CYCBLNK45bl			0		0	54	49	51.5	Normal	30	1.72	0.000014	-0.000004	
CYCBLNK45bO			0		0	39	48	43.5	Normal	30	1.45	0.000012	-0.000004	
CCYC45-1bl	2	1	5.27		7	39.8	39.8	39.8	Normal	0.1	398.00	0.002534	0.002517	
CCYC45-1bO	2	1	5.27		7	28.8	28.9	28.9	Normal	0.3	96.17	0.000615	0.000599	
CCYC45-2bl	1	3	5.27		7	115	115.2	115.1	Normal	0.3	383.67	0.002443	0.002426	
CCYC45-2bO	1	3	5.27		7	38.1	38.6	38.4	Normal	0.3	127.83	0.000816	0.000800	
CCYC45-3bl	1	1	5.27		7	115.9	115.7	115.8	Normal	0.3	386.00	0.002458	0.002441	
CCYC45-3bO	1	1	5.27		7	39.6	40	39.8	Normal	0.3	132.67	0.000847	0.000831	
CCYC45-4bl	2	3	5.27		7	121.8	121.5	121.7	Normal	0.3	405.50	0.002582	0.002565	
CCYC45-4O	2	3	5.27		7	37.9	38	38.0	Normal	0.3	126.50	0.000807	0.000792	
CCYC45-5bl	2	2	5.27		7	48	48.5	48.3	Normal	0.1	482.50	0.003072	0.003054	
CCYC45-5bO	2	2	5.27		7	64.4	64.2	64.3	Normal	1	64.30	0.000412	0.000396	
CCYC45-6bl	1	2	5.27		7	123.4	124.1	123.8	Normal	0.3	412.50	0.002627	0.002609	
CCYC45-6bO	1	2	5.27		7	41.3	41.1	41.2	Normal	0.3	137.33	0.000876	0.000860	
CCYC45-7bl	2	2	5.28		7	53	53.3	53.2	Normal	0.3	177.17	0.001130	0.001112	
CCYC45-7bO	2	2	5.28		7	22.9	22.8	22.9	Normal	0.3	76.17	0.000487	0.000471	
CCYC45-8bl	2	1	5.28		7	130.6	130.3	130.5	Normal	0.3	434.83	0.002769	0.002751	
CCYC45-8bO	2	1	5.28		7	42.6	43.1	43.0	Normal	0.3	143.17	0.000913	0.000898	
CCYC45-9bl	1	3	5.28		7	126.4	125.9	126.2	Normal	0.3	420.50	0.002678	0.002660	

VARIOUS CYCLONE CONFIGURATIONS EXPERIMENT

FILTER NO.	HELIX DESIGN	CYCLONE LENGTH	PARTICLE SIZE (um)	APS PSIZE MEDIAN (um)	FLOW RATE (lpm)	FLUORESCENCE READING CUVET 1	CUVET 2	AVERAGE	PM GAIN	SENSITIVITY RANGE	TRUE READING	CONCENTRATION URANINE (ug/ml)	CORRECTED CONC (ug/ml)	APS CONC (part/cm3)
CCYC45-9bO	1	3	5.28		7	43.8	45	44.4	Normal	0.3	148.00	0.000944	0.000928	
CCYC45-10bl	1	1	5.28		7	126.7	126.4	126.6	Normal	0.3	421.83	0.002686	0.002569	
CCYC45-10b	1	1	5.28		7	48.9	48.7	48.8	Normal	0.3	162.67	0.001037	0.001022	
CCYC45-11bl	1	2	5.28		7	136.2	136.7	136.5	Normal	0.3	454.83	0.002896	0.002878	
CCYC45-11b	1	2	5.28		7	24.3	24.5	24.4	Normal	0.3	81.33	0.000520	0.000504	
CCYC45-12bl	2	3	5.28		7	50.2	50.1	50.2	Normal	0.1	501.50	0.003193	0.003175	
CCYC45-12b	2	3	5.28		7	23.2	23.3	23.3	Normal	0.3	77.50	0.000496	0.000480	
FCBLNK45b2			0	0	0	56	43	49.5	Normal	30	1.65	0.000013	0.000000	0.000
CFC45-1b	2	1	5.27	3.539	14	76.3	76.6	76.5	Normal	0.1	764.50	0.004866	0.004852	0.552
CFC45-2b	1	3	5.27	3.561	14	79	79.5	79.3	Normal	0.1	792.50	0.005044	0.005031	0.536
CFC45-3b	1	1	5.27	3.57	14	79.5	80.2	79.9	Normal	0.1	798.50	0.005082	0.005069	0.535
CFC45-4b	2	3	5.27	3.577	14	83	83.7	83.4	Normal	0.1	833.50	0.005305	0.005291	0.532
CFC45-5b	2	2	5.27	3.589	14	81.1	81.7	81.4	Normal	0.1	814.00	0.005181	0.005167	0.523
CFC45-6b	1	2	5.27	3.59	14	82.8	83.9	83.4	Normal	0.1	833.50	0.005305	0.005291	0.550
CFC45-7b	2	2	5.28	3.598	14	86.1	86.1	86.1	Normal	0.1	861.00	0.005479	0.005466	0.538
CFC45-8b	2	1	5.28	3.595	14	84.2	84.2	84.2	Normal	0.1	842.00	0.005359	0.005345	0.554
CFC45-9b	1	3	5.28	3.605	14	84.6	85.1	84.9	Normal	0.1	848.50	0.005400	0.005387	0.533
CFC45-10b	1	1	5.28	3.605	14	85	85.1	85.1	Normal	0.1	850.50	0.005413	0.005400	0.541
CFC45-11b	1	2	5.28	3.605	14	81.7	82	81.9	Normal	0.1	818.50	0.005209	0.005196	0.546
CFC45-12b	2	3	5.28	3.597	14	83.6	83.9	83.8	Normal	0.1	837.50	0.005330	0.005317	0.517